Transcriptomic Analysis Reveals Metabolic and Epigenomic Reprogramming During Lytic Phase of MHV-68 Infection

Chloe Jones

A dissertation

submitted in partial fulfillment of the

requirements for the degree of

Doctor of Philosophy

University of Washington

2025

Reading Committee:

Thelma Escobar, Chair

Andrea Wills

Alex Merz

Program Authorized to Offer Degree:

Biochemistry

University of Washington

Abstract

Transcriptomic Analysis Reveals Metabolic and Epigenomic Reprogramming During Lytic Phase of MHV-68 Infection

Chloe Jones

Chair of the Supervisory Committee:

Thelma Escobar

Biochemistry

The human gammaherpesviruses (γHV) Kaposi Sarcoma-Associated Virus (KSHV) and Epstein Barr Virus (EBV) are two of the seven known human oncogenic viruses. KSHV infects around 5% of the population and causes cancers such as Kaposi Sarcoma in immunodeficient individuals, whereas EBV infects >90% of the population and is linked to lymphomas and, more recently, multiple sclerosis. Despite their impact on human health, there are currently no drugs to treat either virus. This may in part be due to difficulties studying the lytic phase in the human γHVs; KSHV and EBV both immediately enter latency upon initial infection. A better understanding of what processes occur during the lytic phase, the part of the viral lifecycle during which the virus actively replicates, may offer new insights on potentially druggable pathways. MHV-68 is a murine γHV that immediately enters the lytic phase upon primary infection and shares ~80% sequence similarity with the human γHVs, thus making it a good model for studying the lytic phase in the human γHVs. Surprisingly, there have been no prior studies of the host transcriptome during viral infection of NIH3T3 cells, one of the most common models for the study of MHV-68. In this body of work, I analyze bulk RNA-seq data from MHV-68 infected NIH3T3 cells with the goal of identifying potential druggable pathway(s). In taking a two-pronged approach in which I assess the most differentially expressed metabolic and epigenomic genes/pathways, I present transcriptomic evidence for increased redox stress in MHV-68 infected NIH3T3 cells, as well as evidence for perturbations in chromatin biology. My analysis indicated an increase in transcripts encoding components of the mitochondrial electron transport chain, glutathione synthesis, and NADPH-producing pathways, collectively suggesting increased oxidative stress over the course of infection. Notable changes in chromatin biology include upregulation of the expression of DNA demethylases and the DNA damage response chaperone DAXX. Additionally, canonical histone H2A was upregulated, while histone variant H2AX was downregulated late in lytic infection. Ultimately, I found that inhibition of the DNA demethylating enzymes Ten-eleven translocase 1 and 2 (Tet1 and Tet2) diminishes MHV-68 replication in this system. The mechanism behind how Tet1/2 inhibition reduces viral titer remains to be explored.

CHAPTER 1: BACKGROUND

CHAPTER 2: RESULTS

CHAPTER 3: IMPLICATIONS AND FUTURE DIRECTIONS

1. INTRODUCTION

1.1 Impact of Gammaherpesviridae on Human Health

Herpesviruses are common pathogens that collectively infect the majority of humans worldwide[1]. They are known for being incurable, which they achieve by associating with their host's genome, replicating when their host cell does. This allows them to remain dormant for many years, with the potential to reactivate later. Therefore, herpesviruses have the potential to cause both acute infection and long-term complications to the host, including cancer and multiple sclerosis.

Gammaherpesviruses (γHVs) are a clade of herpesvirus that integrate into the host genome through formation of a circular structure known as an episome, which is tethered to the host chromosomes by a viral protein[2]. There are two γHVs that infect humans: Kaposi sarcoma-associated virus (KSHV) and Epstein-Barr virus (EBV). KSHV infects ~5% of the US population[3-5]. While symptoms of acute infection are rare in immunocompetent individuals, infection with KSHV can cause a variety of cancers, including a variety of lymphomas, multicentric Castleman's disease, and Kaposi sarcoma[6]. These diseases are especially prevalent in immunocompromised individuals, for instance, in those with acquired immunodeficiency syndrome or in transplant patients. EBV infects >90% of the global adult population[7,8] and is also known to cause cancer, including lymphomas as well as nasal and gastric carcinomas. More recently, strong evidence has arisen that EBV may also cause multiple sclerosis (MS) in a small subset of the population it infects[9,10]. Despite the burden of disease, there are currently no FDA recommended treatments for gammaherpesviral infections. Development of therapeutics for gammaherpesviral infection could impact human health by reducing the incidence of the aforementioned cancers, or even potentially preventing or treating MS.

Developing a treatment for herpesviral infection is limited by the narrow host specificity of herpesviruses. Human herpesviruses are not known to infect other species, and it is rare for herpesviruses in general to cause infections across multiple species[11]. Models for studying the human γHVs are thus limited to tissue culture, the use of humanized animal models, or the use of model γHVs with their natural hosts. The

murine herpesvirus MHV-68 shares ~80% of its protein coding genes with EBV and KSHV[12] and infects similar cell types, making it an appropriate model for studying the human γHVs.

The study of γHVs is further complicated by the viral lifecycle. As mentioned above, γHVs associate with the host genome and can remain dormant; this is the latent phase of the lifecycle[13]. In contrast, during the lytic phase the virus replicates independently of host genome replication. The processes that occur during each phase are distinct; different viral proteins are expressed during different phases of the lifecycle, with host cellular processes also being differentially affected.

KSHV and EBV both infect epithelial and B cells; KSHV can additionally infect endothelial cells. MHV-68 can similarly infect epithelial and B cells, but it has additionally been observed to affect macrophages and dendritic cells[14-17]. To attach to their target cell, all herpesviruses require viral glycoproteins gB, gH, and gL. KSHV and EBV are no different, though they have been noted to require additional factors for viral attachment[13]. EBV additionally requires viral protein BMRF to attach to the epithelial receptor EphA2, whereas attachment to B cells involves gp350 binding to CR2/CD21 receptors. Less is known about the receptors involved in attachment of KSHV, though it has been noted to use EphA2 as well as EphA4. Less is known about viral fusion. In EBV infection of B cells, fusion is triggered by viral protein gp42 binding to cell surface HLA-II. In KSHV infection of B cells, evidence suggests viral protein K8.1A is required for viral entry, but not much else is known about factors required for fusion. Neither the viral nor the host receptors required for attachment or fusion are known for MHV-68. However, it is known that KSHV, EBV, and MHV-68 all enter the cell via some form of endocytosis[18-20]. Little is known about the dynamics of KSHV and EBV viral particles post-fusion, but there have been studies in MHV-68 as well as other clades of herpesviruses. In an electron tomography (ET) study of MHV-68 dynamics[20], it was noted that the viral envelope is dissolved in as soon as 20 minutes post-infection. Viral capsids were then observed to cluster around nuclear pores and inject their DNA into the host nucleus. When the virus replicates, the viral capsid is assembled in the nucleus and exported by envelopment in the inner nuclear membrane, followed by fusion and de-envelopment with the outer nuclear membrane, releasing a naked capsid into the cytoplasm. From there, it develops two layers of tegument before envelopment by budding

into Golgi-derived membrane structures. Viral particles were reported to be found in exocytic vesicles as soon as 24 hours post-infection (24hpi).

The processes observed in MHV-68 are similar to those seen in the alphaherpesvirus herpes simplex virus 1 (HSV-1)[21], which indicates that they are likely conserved across all herpesviruses. One notable exception to this is that HSV-1 is known to utilize the host microtubule system to transit to the nucleus, but there was no mention of the microtubule network in the aforementioned ET study of MHV-68[20]. However, there is evidence that KSHV requires microtubule networks for transit to the nucleus[22]. EBV and KSHV have a strong preference to establish latency upon primary infection[13]. Neither virus forms plaques on cultured cells, and neither will enter the lytic phase in culture without external manipulation[23,24]. In contrast, MHV-68 preferentially enters the lytic phase during primary infection in culture. This makes MHV-68 ideal as a model for the study of the lytic phase in γHVs. Despite this, to the best of our knowledge, the host transcriptome has never been sequenced during MHV-68 infection in NIH3T3 cells, a very common model for studying MHV-68 pathogenesis. Sequencing the transcriptome over a timecourse of MHV-68 infection will bring potential druggable pathways to light.

In our analyses of the transcriptome during MHV-68 infection, we focused on two broad pathways: metabolism and epigenetic modifications. Many currently available antiviral drugs, including those targeting alpha- and beta- herpesviruses, target metabolic pathways[25]. For example, Acyclovir is used to treat both HSV and varicella zoster virus (VZV), two human alphaherpesviruses. Acyclovir is a prodrug. The active form is a nucleoside analog that causes chain termination during viral DNA replication, preventing the virus from replicating. While there are currently no approved antiviral drugs that target chromatin, there are FDA-approved drugs targeting chromatin modifying proteins. One such drug is Vorinostat, which treats T cell lymphoma by targeting class I and II histone deacetylases[26]. Additionally, many groups are currently investigating the use of chromatin-targeting drugs to treat latent viral infections, including herpesviruses[27]. Details regarding what is already known about metabolomics and epigenomics in gammaherpesviral infection will be discussed in the sections below.

1.2 Metabolomics of Gammaherpesviridae

Viruses hijack their hosts' machinery in order to replicate themselves. Naturally, this means they must exert some control over expression of host metabolic enzymes and transport proteins. Studies from the mid twentieth century indeed confirmed that viral infection induces metabolic changes in this host, but despite this, the field of viral metabolomics didn't take off until widespread adoption of appropriate mass spectrometry pipelines at the turn of the twentieth century[28,29]. Viral metabolomics has since become a topic of interest, with the field converging on the idea that viruses tend to remodel a common set of metabolic pathways during infection, towards similar ends. For example, viruses all require nucleotides (either RNA or DNA) and protein synthesis in order to replicate themselves, and these processes have also been found to be upregulated and coopted in a variety of viral infections. Many viruses have also been demonstrated to induce the Warburg effect, also known as aerobic glycolysis[28,29]. The Warburg effect, best known in the context of cancer, is the upregulation of glycolysis and the production of lactic acid in an aerobic environment. While an inefficient use of glucose in the long-term, this process provides ATP to the cell quickly in the short-term; given that viruses tend to destroy the host cell over the long-term, it makes sense that viral infection would induce the Warburg effect.

Previous work indicates that the γHVs share many of these common patterns, which I discuss in detail below. In the meantime, it is important to note a few particulars that may impact interpretation of the results in my system (MHV-68 infection of NIH3T3 cells) compared to the current body of literature. First, because it is difficult to study lytic infection without artificially inducing it, most data on KSHV and EBV metabolomics focuses on the latent phase of the viral lifecycle. Further confounding analysis of results, studies use a variety of different models that confound our ability to draw confluent conclusions. EBV, KSHV, and MHV-68 are all capable of infecting both B cells and endothelial cells. In publications that use models of infection that do not progress to cancer, those that focus on KSHV tend to use endothelial or epithelial cell-derived models such as telomerase reverse transcriptase (TERT)-immortalized dermal microvascular endothelial cells[30,31], oral epithelial cells[32], or even rat endothelial cells[33,34]. This is likely due to the fact that KSHV is most well-known for causing an endothelial-derived cancer, the eponymous

Kaposi Sarcoma. In contrast, studies evaluating metabolic changes during EBV infection are more likely to use primary B human cells[35-37].

The human γHVs follow many of the trends established for viral metabolic perturbations. In particular, they have been noted to: exhibit the Warburg effect; upregulate nucleotide biosynthesis, including the pentose phosphate pathway (PPP); increase glutaminolysis to anaplerotically provide carbon to the tricarboxylic acid cycle; and upregulate fatty acid (FA) synthesis, likely to provide FAs for the viral envelope[28,29] (**Fig 1**). While these studies have largely been done in latently infected cells, a few have reached similar conclusions about the same pathways being important during the lytic phase, at least in KSHV[31]. In the following paragraphs, I will describe what is known about each of these major processes.

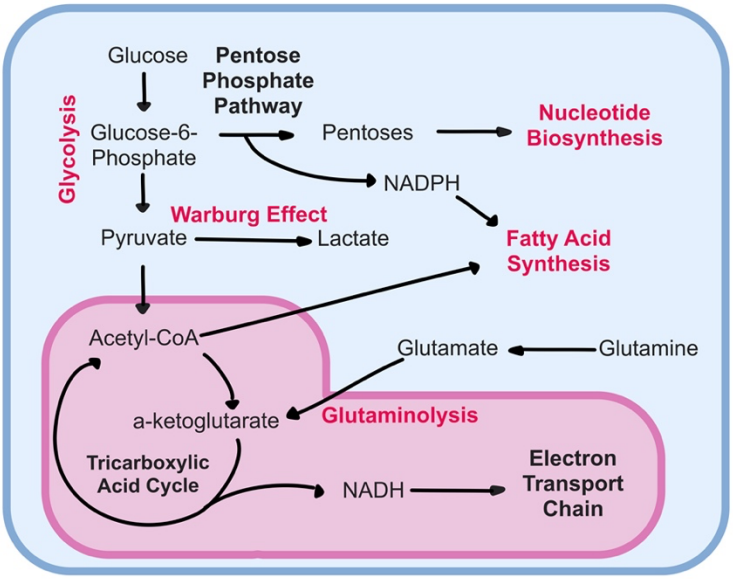

Figure 1. Schematic of relevant metabolic pathways. Pathways previously indicated to be active in the human gammaherpesviruses are highlighted in red. Pathway names are in bold. Only relevant metabolites are named; the entire pathways are not shown.

Most reports indicate that glycolysis is upregulated in EBV[37] and KSHV infection[31]. Furthermore, in models meant to recapitulate cancer biology both γHVs, it has been found that infection induces the Warburg effect, including an increase in lactate production[38-40]. However, an increase in oxidative phosphorylation is also observed in EBV in the same cellular contexts[35,37]. At least one report indicates

that KSHV downregulates oxidative phosphorylation in endothelial cells[38], but there are also reports that, in B cells, it increases reactive oxygen species (ROS), of which oxidative phosphorylation is a major source[41,42]. In summary, repeated observation of the Warburg effect indicates that both human γHVs use carbohydrates as their primary source of energy during latency. EBV also induces increased oxidative phosphorylation, while evidence for oxidative phosphorylation occurring in KSHV infection is inconclusive and potentially cell-type dependent.

While carbohydrates appear to be the primary source of *energy* for γHV infected cells, they may not be the primary source of carbon skeletons. Glutaminolysis, the process by which certain amino acids are converted into alphaketoglutarate to be anapleurotically fed into the TCA cycle, has also been found to be upregulated in cells infected by alpha-, beta- and γHVs[28,29]. In the betaherpesvirus HCMV, specifically, it has been indicated that, while labelled glucose does not accumulate in the TCA cycle[43], labeled glutamine does[44]. This implies that glutamine is the primary source of carbon for the TCA cycle in HCMV, with this feature potentially being shared throughout the clade. Indeed, glutamine has been reported to be necessary for cell survival and viral protein expression during KSHV infection[28,31,45]. In EBV, induction of glutaminolysis has been linked to the viral protein LMP1[46,47,48].

Nucleotide biosynthesis is also important in viral infection. For γHVs, both purine and pyrimidine biosynthesis has been demonstrated to be upregulated during infection, but purines appear to be more important. One publication indicated that, while purine and pyrimidine pathways showed similar levels of enrichment at a transcriptional level, their mass spectrometry quantified metabolomics dataset indicated that purine intermediates were more abundant at most timepoints[49]. Supporting the notion that purine synthesis is particularly important, formate[37] and xanthine[32], two intermediates used in the synthesis of purines, were found to be more abundant during latency in EBV and KSHV, respectively. In the case of formate, it was also specifically found that a major source of formate during EBV infection is serine. Serine also is converted into glycine, with much of that glycine shunted into the synthesis of glutathione[37].

Herpesviruses are enveloped viruses; they therefore require lipids for envelope assembly. Indeed, lipid metabolism has been reported to be important for the betaherpesvirus cytomegalovirus[43,50] and the alphaherpesvirus HSV-1[51-53]. Multiple reports have also indicated that lipid and cholesterol biosynthesis is important for γHVs, specifically. Inhibiting fatty acid synthesis (FAS) in latently KSHV infected tert-immortalized endothelial (TIME) cells induces apoptosis[30]. This group used TOFA to inhibit the production of malonyl CoA by acetyl CoA carboxylase, the first step in the FAS pathway. They found that supplementation with palmitic acid partially rescued cell death, indicating that. A similar report in KSHV used both TIME cells and a cell line that induces KSHV **lytic** replication upon doxycycline supplementation showed that inhibiting FAS not only induces apoptosis, but also decreases virion production. In EBV infection of primary B cells, it has been shown that both FAS and cholesterol synthesis are strongly upregulated at 2 days postinfection, and continue to be upregulated throughout the establishment of latent infection[36]. Furthermore, the same study found that treatment with simvastatin, an HMG-CoA reductase inhibitor, reduced cell proliferation. This group was also further able to show that it was specifically the isoprenoid branch of the cholesterol pathway that is necessary for the virus to achieve optimal growth.

There are few reports that have addressed the metabolome in MHV-68 specifically. One metabolomics study, also in NIH3T3 cells, indicates that glutamine metabolism, lipid biogenesis, and glycolytic pathways were upregulated at various time points post lytic infection[54]. We plan to characterize the transcriptome in this same system to complement this metabolomic data. Specifically, one of my goals is to validate MHV-68 as a good model for studying metabolism in the human γHVs; if we see patterns in metabolic gene expression during MHV-68 infection that match what is known of KSHV and/or EBV, then this would support that conclusion. If we validate MHV-68 as a good model, another goal is to find a preliminary drug target.

1.3 General Principles of Chromatin Biology

The term “chromatin” refers to the DNA-protein complex formed when DNA is wrapped around histones to compact it (**Fig 2**). Without compaction, the length of a single human cell’s diploid genome would be

about 2 meters long and therefore would not be able to fit within the nucleus[55]. However, not all regions of the genome are compacted to the same extent; some regions are much denser than others and are thus much transcriptionally inaccessible. These regions are dubbed “heterochromatin.” Regions of the genome that are transcriptionally accessible are called “euchromatin.” Differences in density between euchromatin and heterochromatin are so stark, they can be visualized via transmission electron microscopy[56].

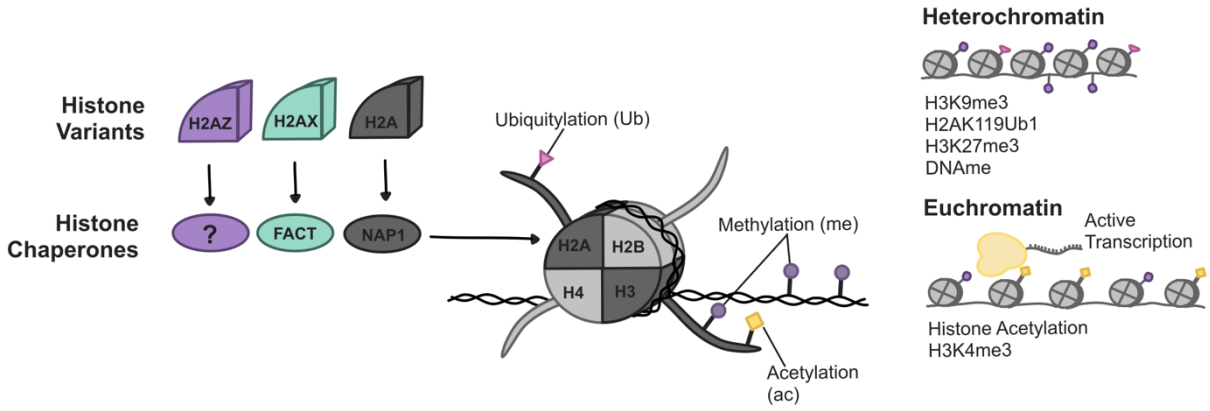

Figure 2. Schematic showing chromatin-related factors that are explored in this work. The nucleosome is composed of an octamer of four core histones: histones H2A, H2B, H3, and H4. Histones H2A and H3 have many isoforms, called “variants;” depicted here are H2A variants already postulated to be important in gammaherpesviral infection. Histone chaperones help assemble the nucleosome-DNA complex. Histones can also be post-translationally modified with a variety of chemical groups, most notable here being methylation, acetylation, and ubiquitylation. Additionally, DNA can be methylated. Together, these factors help modulate chromatin state. Chromatin exists either as transcriptionally accessible euchromatin or transcriptionally inaccessible heterochromatin. Factors associated with each state are indicated.

Chromatin modulates gene expression by controlling access of the transcriptional machinery to DNA. It achieves this by differentially compacting different regions of the genome in different cell types/ contexts. To “open” chromatin, remodeling complexes such as the BAF complex physically move nucleosomes[57,58] and have been associated with changes in chromatin state[59-61]. Specifically, the BAF complex is known to evict nucleosomes[62,63] and oppose the action of the heterochromatin-associated Polycomb Repressive

Complexes (PRC)[64,65]. In contrast, packing into dense heterochromatin is achieved by accessory proteins such as heterochromatin-associated protein 1 (HP1)[66]. The histone post-translational modification (H-PTM) histone 3 lysine 9 trimethylation (H3K9me3; similar structural nomenclature will be used for other discussed H-PTMs) recruits HP1[67]. Two other H-PTMs are associated with heterochromatin: H3K27me3 and H2AK119 monoubiquitylation (H2AK119Ub1), deposited by PRC2 and PRC1, respectively. While the association between these marks and heterochromatin has been well characterized, the mechanism behind how these marks achieve chromatin compaction is debated[68-70]. Other H-PTMs are associated with active transcription and euchromatin; this includes H3K4me1, H3K4me3, and H3K36me3[71]. Each of these are associated with a different region of the gene body/ promoter region. Histone acetylation in general is also associated with chromatin accessibility, as the negative charge possessed by the acetyl group in biological conditions neutralizes the positive charge of histone lysine residues[72]. Many more H-PTMs exist, including other methylation marks, ubiquitylation marks, phosphorylation, and more[71] but their functions are either not thought to be related to chromatin accessibility or they are currently not as well characterized.

Other factors shaping chromatin dynamics include histone chaperones, DNA methylation, and histone variants. Histone chaperones are proteins that are involved in packaging histones in chromatin, whether this be in the context of replication or the regular growth of the cell, and include members such as Caf1, Asf1, and Npm1. DNA methylation typically occurs at CpG islands and is associated with gene repression, as well as certain H-PTMs. The DNA methyltransferase (DNMT) family transfers methyl groups to DNA, whereas the ten eleven translocase (TET) family is involved in removing DNA methylation. In addition to the level of regulation offered by H-PTMs, the core histones H3 and H2A also have a variety of isoforms that can serve specific functions within the cell. These isoforms are commonly termed “histone variants.” Histone variant H2Ax, which will be discussed later, is known to be associated with DNA damage responses[73].

1.4 Chromatin Dynamics in Gammaherpesviral Infection

Viruses have a variety of reproductive strategies. Many double-stranded DNA viruses insert themselves into their host's genome; this is true for the herpesviruses, which chromatinize their genomes into structures called episomes during the latent phase of infection[74]. In this context, "chromatinization" is the process of condensing the viral genome around host histones.

One histone variant in particular has been thoroughly researched in γHVs. H2AX has been shown to be important for KSHV proliferation; specifically, knockdown or knock out of H2AX results in lower viral titers[75,76]. H2AX has been associated with DNA damage responses[77] and it has thus been postulated that gH2AX may be recruited in response to DNA damage caused by the virus. It has also been noted that in KSHV, H2AX associates with viral LANA, the protein responsible for tethering the episome to the host genome[75]. This indicates that H2AX may be involved in the proper tethering of the viral episome of the host genome. V-68 and EBV have their own virally-encoded kinases that phosphorylate H2AX[76]. Interestingly, a more recent publication showed that a different H2 variant, H2AZ, associates with the EBV episome tethering protein EBNA1[77]. The precise function of both of these H2 variants in chromatinized γHV genomes has yet to be fully explored.

While in the latent phase, it has been found that not only are host histones added to viral DNA, but that specific histone modifications are present at certain genomic regions[78,79]. This indicates that γHVs may be exploiting the host's chromatin regulatory mechanisms to regulate access at specific points in its own genome. The H-PTMs found decorating γHV episomes during latency include H3K27me3, H3K9me3, H3K4me3, among others[78,79]. In one study that was focused on lytic reactivation from latency in KSHV, the genes associated with the earliest expression on lytic reactivation tended to have a bivalent H3K27me3 + H3K4me3 signature, whereas genes that are expressed later in reactivation tended to only have repressive H3K27me3 or H3K9me3[78]. This study also found that inhibition of H3K27me3 deposition led to lytic reactivation of KSHV.

In addition to herpesviruses chromatinizing their genomes, they can also induce changes to *host* chromatin. In a particularly dramatic example, HSV-1 lytic replication pushes the host genome to the nuclear periphery[80]. For γHVs, EBV is also known to modify its host's genome in a variety of ways. Widespread host DNA demethylation has been observed during the latent phase[81,82], as has a decrease in repressive histone marks H3K9me3 and H3K27me3 on host DNA[83], which may indicate a global increase in transcription as the virus reprograms its target cell. To my knowledge, there are currently no studies addressing how γHVs may modify the host's chromatin during the lytic phase.

We know somewhat more about what happens to the episome during the lytic phase. During viral replication/ the lytic phase, it appears that histones dissociate from the viral genome[78,80,84], likely to make the viral genome maximally accessible for transcription. Histone evicting complexes and/or histone chaperones may be involved in this de-chromatinization process, but data on these proteins during the lytic phase of infection is scarce. I have used MHV-68 as a model to study the lytic phase, and anticipate that my work will to add to the body of knowledge around general chromatin dynamics during lytic infection by γHVs.

2. RESULTS

2.1 Brief Explanation of Methods

This was a collaboration with Tracie Delgado's group at Seattle Pacific University in which they conducted the infection and RNA processing while I performed the computational processing. We collaborated on data analysis. Briefly, NIH3T3 cells, a murine fibroblast cell line, were infected with MHV-68 and harvested at 4, 8, 12, and 24 hours post infection (hrpi). We included a time-paired mock control. Four replicates were prepared. RNA was harvested and purified with a miniprep kit and converted to cDNA using poly-A primers. The computational pipeline used Fastqc for quality check, STAR to align, salmon to quantify, and DESeq2 for differential expression analysis. Additional details can be found in the materials and methods section below.

2.2 Statistics/ Data Analysis

We performed four replicates for each condition (mock/infected, 4/8/12/24 hours post-infection). Upon performing a principal component analysis (PCA), samples from the same treatment clustered together (**Fig 3A**). The number of significantly differentially expressed (DE) genes increased as the infection progressed, as visualized via volcano plots generated for the four tested timepoints (**Fig 3B**). Key genes relating to viral immune response, including Mx2 and Ifit1, were upregulated, supporting our experimental setup and analysis.

At 4hpi, 8% (3274/40413) of transcripts were DE; by 24hpi, 22% (8847/40413) of transcripts were DE (**Fig 3C**). This is a huge proportion of the genome that has been perturbed by infection, but it is not entirely surprising. ~31% of genes DE at 4hpi remained DE throughout infection; similarly, 38% (2041/5428) of genes DE at 8hpi are maintained as DE until 24hpi. In contrast, ~26% of genes DE at 24hpi were differentially expressed at that timepoint, specifically. This indicates that the virus systematically rewires the host transcriptome over time, with many genes exhibiting DE by 4hpi and maintaining that DE at least up until the final timepoint assessed at 24hpi.

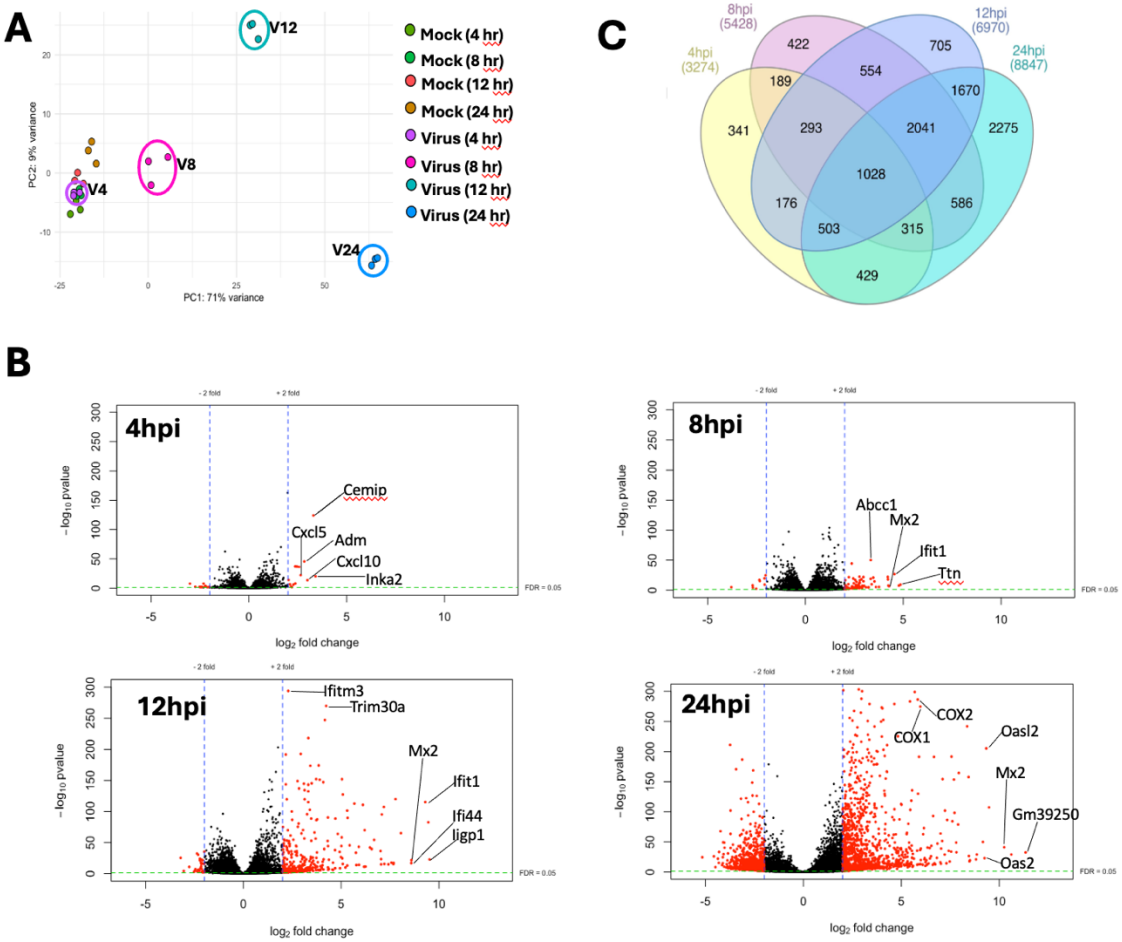

Figure 3. MHV-68 progressively perturbs the NIH3T3 cell transcriptome, expressing viral response genes. A) Principal component analysis (PCA) plot of all samples. **B)** Volcano plots for 4, 8, 12, and 24 hours post-infection (hpi). Points highlighted in red meet the following criteria: adjusted p value ≤ 0.05, log2 fold change ≥ 2. Selected genes are also indicated. **C)** Venn diagram showing genes that are significantly differentially expressed, and which timepoints they are differentially expressed in. Genes in this plot meet the following criteria: adjusted p ≤ 0.05.

2.3 Transcription Factor Analysis

I next performed an unbiased analysis of transcription factor target genes using RegNetwork's transcription factor (TF) network database. The eight gene sets I evaluated were those significantly up and downregulated at 4hpi, 8hpi, 12hpi, 24hpi. All genes in this analysis met the following criteria: p value ≤ 0.05, log2 fold change ≥ 0.5.

At 4hpi, targets of Hif1a and Trp53 (protein name p53) were upregulated (**Fig 4**). Notably, Hif1a has been reported to be induced in both KSHV and EBV infection[85-87], while p53 signaling has been noted to be manipulated by both KSHV and EBV[88,89]. Interestingly, targets of the Mcm helicase family, required for host DNA replication, are upregulated at 8hpi, but downregulated at 12 and 24hpi. Foxm1 and Espl1 targets were both enriched and had a high -log10 FDR in the group of genes upregulated at 12hpi. Foxm1 is involved in regulating cell proliferation, apoptosis, and lipid and carbohydrate metabolism[90], as well as being a commonly misregulated protein in the context of cancer[91]; indeed, it has been specifically noted to be upregulated in cases of Kaposi Sarcoma, a cancer caused by the human γHV KSHV[92]. Espl1 encodes separase, a protein that cleaves cohesin to initiate anaphase. In the group of genes downregulated at 8hpi, HoxC8 target genes were enriched, with a high -log10 FDR. HoxC8 is one of the homeobox genes and is broadly involved in cell proliferation and differentiation. Among genes significantly upregulated at 12hpi, Irf7 was the third most enriched and had a high -log10 FDR. Genes upregulated at 24hpi were enriched for factors involved in transcription by RNA polymerase II (RNApol II), including RNApol II subunits themselves. This may indicate an enrichment of RNA pol II targets over targets of other RNA polymerases.

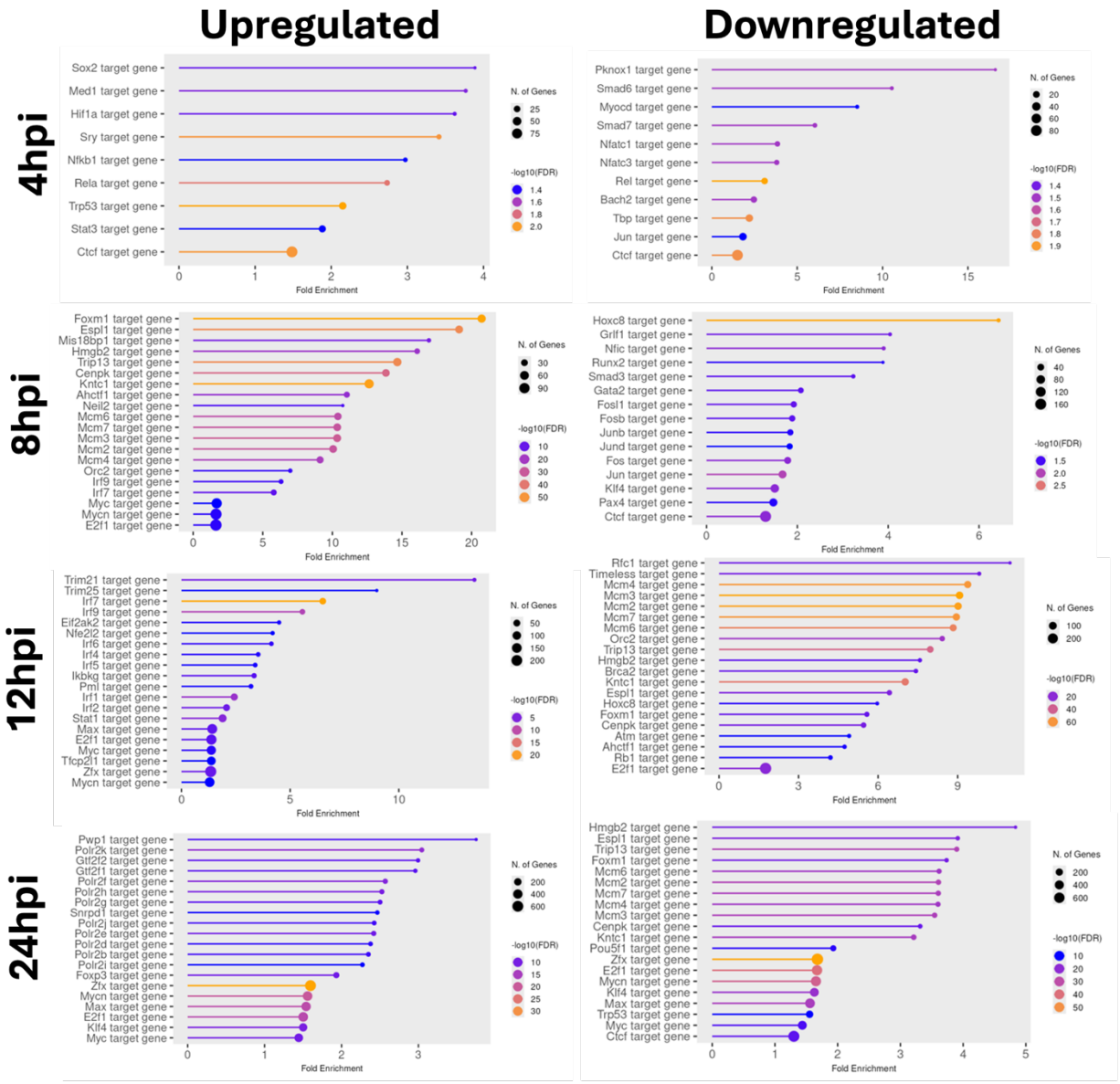

Figure 4. Transcription factor targets are differentially regulated upon viral infection, and different transcription factor networks are active at different timepoints in infection. Enrichment of transcription factor targets in gene sets specifically expressed at conditions indicated. Keys for FDR and pathway gene number are indicated to the right of each individual plot. Gene lists were filtered for the following criteria: adjusted p value of <0.05; log2 fold change of >|0.5|; baseMean of >30.

2.4 Unbiased Pathway Analysis

I next performed an unbiased pathway analysis using Kyoto Encyclopedia of Genes and Genomes (KEGG) and Gene Ontology: Biological Process (GO:BP) databases[139,140]. I chose these databases because they seemed most appropriate for identifying a druggable target in terms of cellular pathways (KEGG) or biological processes (GO:BP).

In the KEGG pathway analysis (**Fig 5A**), a variety of virus-related pathways are enriched in upregulated genes across timepoints. Viral interaction with cytokine and cytokine receptor is upregulated at 4hpi; COVID-19 and EBV infection pathways are upregulated at 8hpi; COVID-19, HSV-1, and KSHV infection pathways are upregulated at 12hpi; and HSV-1 related-pathways are represented at 24hpi. Other pathways shared across timepoints include ferroptosis and glutathione metabolism. Ferroptosis is a process of cell death that requires iron and is characterized by lipid peroxidation and oxidative stress[93]. Reduced glutathione acts as an antioxidant; specifically, it donates electrons to reactive oxygen species, neutralizing them[94]. Ferroptosis is enriched at 4 and 8hpi, whereas glutathione metabolism is upregulated at 8 and 12hpi.

While some processes are shared across different timepoints, others are distinct. At 4hpi, a variety of signaling pathways were identified as upregulated: p53, Hippo, Rap1, and TNF signaling were all enriched. At 8hpi, cell cycle and ribosome pathways were enriched in the group of upregulated genes. Moving into 12hpi, pathways directly relating to response to viral infection are enriched in the upregulated subset of genes: RIG-I-Like signaling, cytosolic DNA sensing, and antigen processing and presentation are upregulated. Finally, at 24hpi, aminoacyl tRNA biosynthesis, RNA degradation, and mRNA surveillance pathways are upregulated.

While many signaling pathways were identified as upregulated at 4hpi, MAPK signaling was downregulated. In the group of genes downregulated 8hpi, biosynthesis of nucleotide sugars and amino sugar metabolism were the top two enriched pathways, albeit with low -log10 FDR. Otherwise, pathways relating to cell adhesion such as ECM-receptor interaction and focal adhesion were enriched with higher -

log10 FDR. This is notable because of the use of endothelial cells for our experiment; downregulation of these pathway members could be an indication of a loss of cellular identity or cytopatholgy at the transcriptional level. At 12hpi, a variety of pathways relating to DNA replication and repair were downregulated: DNA replication, mismatch repair, homologous recombination, Fanconi anemia, and base excision repair were all represented here. Curiously, at 24hpi both oxidative phosphorylation and chemical carcinogenesis reactive oxygen species pathways were both downregulated.

The GO:BP pathway analyses largely recapitulate the KEGG pathway analyses (**Fig 5B**). At 4hpi, pathways relating to differentiation are upregulated, while pathways relating to cell-cell adhesion are downregulated. Again, this is likely a reflection of broad transcriptional rewiring in the NIH3T3 cells. At 8hpi, pathways relating to meiosis and chromatid segregation are upregulated. Proceeding to 12hpi, upregulated pathways include many involved in viral responses; this is in line with the KEGG analysis indicating the most antiviral response at this time. Pathways relating to DNA replication and mismatch repair are downregulated at this timepoint, also in support of the KEGG analysis. Finally, upregulated pathways at 24hpi are also enriched for RNA and nucleic acid processing and synthesis.

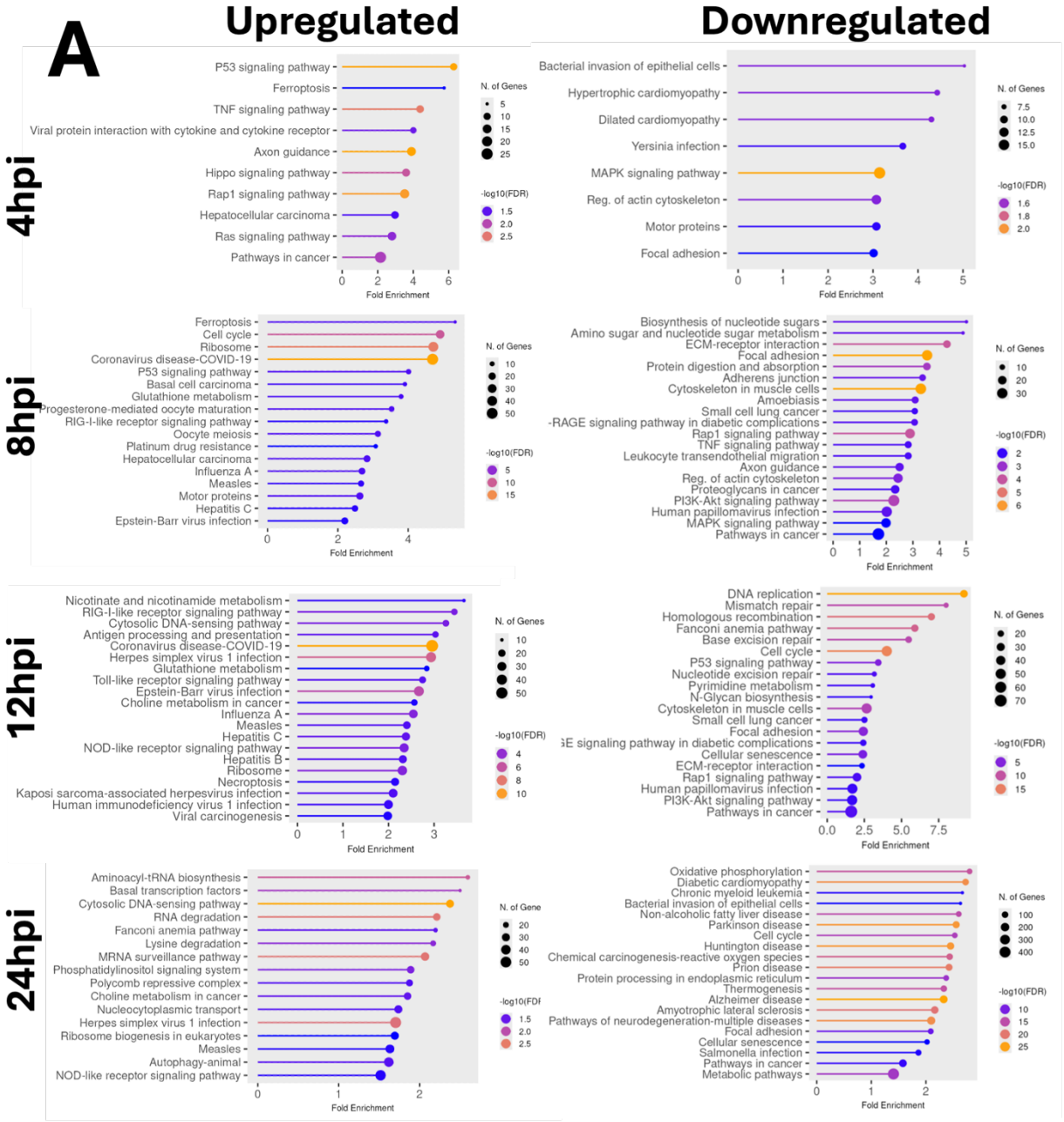
A
Upregulated
Downregulated
4hpi
P53 signaling pathway
Ferroptosis
TNF signaling pathway
Viral protein interaction with cytokine and cytokine receptor
Axon guidance
Hippo signaling pathway
Rap1 signaling pathway
Hepatocellular carcinoma
Ras signaling pathway
Pathways in cancer
Fold Enrichment
N. of Genes
-log10(FDR)
Bacterial invasion of epithelial cells
Hypertrophic cardiomyopathy
Dilated cardiomyopathy
Yersinia infection
MAPK signaling pathway
Reg. of actin cytoskeleton
Motor proteins
Focal adhesion
8hpi
Ferroptosis
Cell cycle
Ribosome
Coronavirus disease-COVID-19
P53 signaling pathway
Basal cell carcinoma
Glutathione metabolism
Progesterone-mediated oocyte maturation
RIG-I-like receptor signaling pathway
Oocyte meiosis
Platinum drug resistance
Hepatocellular carcinoma
Influenza A
Measles
Motor proteins
Hepatitis C
Epstein-Barr virus infection
Biosynthesis of nucleotide sugars
Amino sugar and nucleotide sugar metabolism
ECM-receptor interaction
Focal adhesion
Protein digestion and absorption
Adherens junction
Cytoskeleton in muscle cells
Amoebiasis
Small cell lung cancer
-RAGE signaling pathway in diabetic complications
Rap1 signaling pathway
TNF signaling pathway
Leukocyte transendothelial migration
Axon guidance
Reg. of actin cytoskeleton
Proteoglycans in cancer
PI3K-Akt signaling pathway
Human papillomavirus infection
MAPK signaling pathway
Pathways in cancer
12hpi
Nicotinate and nicotinamide metabolism
RIG-I-like receptor signaling pathway
Cytosolic DNA-sensing pathway
Antigen processing and presentation
Coronavirus disease-COVID-19
Herpes simplex virus 1 infection
Glutathione metabolism
Toll-like receptor signaling pathway
Epstein-Barr virus infection
Choline metabolism in cancer
Influenza A
Measles
Hepatitis C
NOD-like receptor signaling pathway
Hepatitis B
Ribosome
Necroptosis
Kaposi sarcoma-associated herpesvirus infection
Human immunodeficiency virus 1 infection
Viral carcinogenesis
DNA replication
Mismatch repair
Homologous recombination
Fanconi anemia pathway
Base excision repair
Cell cycle
P53 signaling pathway
Nucleotide excision repair
Pyrimidine metabolism
N-Glycan biosynthesis
Cytoskeleton in muscle cells
Small cell lung cancer
Focal adhesion
GE signaling pathway in diabetic complications
Cellular senescence
ECM-receptor interaction
Rap1 signaling pathway
Human papillomavirus infection
PI3K-Akt signaling pathway
Pathways in cancer
24hpi
Aminoacyl-tRNA biosynthesis
Basal transcription factors
Cytosolic DNA-sensing pathway
RNA degradation
Fanconi anemia pathway
Lysine degradation
MRNA surveillance pathway
Phosphatidylinositol signaling system
Polycomb repressive complex
Choline metabolism in cancer
Nucleocytoplasmic transport
Herpes simplex virus 1 infection
Ribosome biogenesis in eukaryotes
Measles
Autophagy-animal
NOD-like receptor signaling pathway
Oxidative phosphorylation
Diabetic cardiomyopathy
Chronic myeloid leukemia
Bacterial invasion of epithelial cells
Non-alcoholic fatty liver disease
Parkinson disease
Cell cycle
Huntington disease
Chemical carcinogenesis-reactive oxygen species
Prion disease
Protein processing in endoplasmic reticulum
Thermogenesis
Alzheimer disease
Amyotrophic lateral sclerosis
Pathways of neurodegeneration-multiple diseases
Focal adhesion
Cellular senescence
Salmonella infection
Pathways in cancer
Metabolic pathways

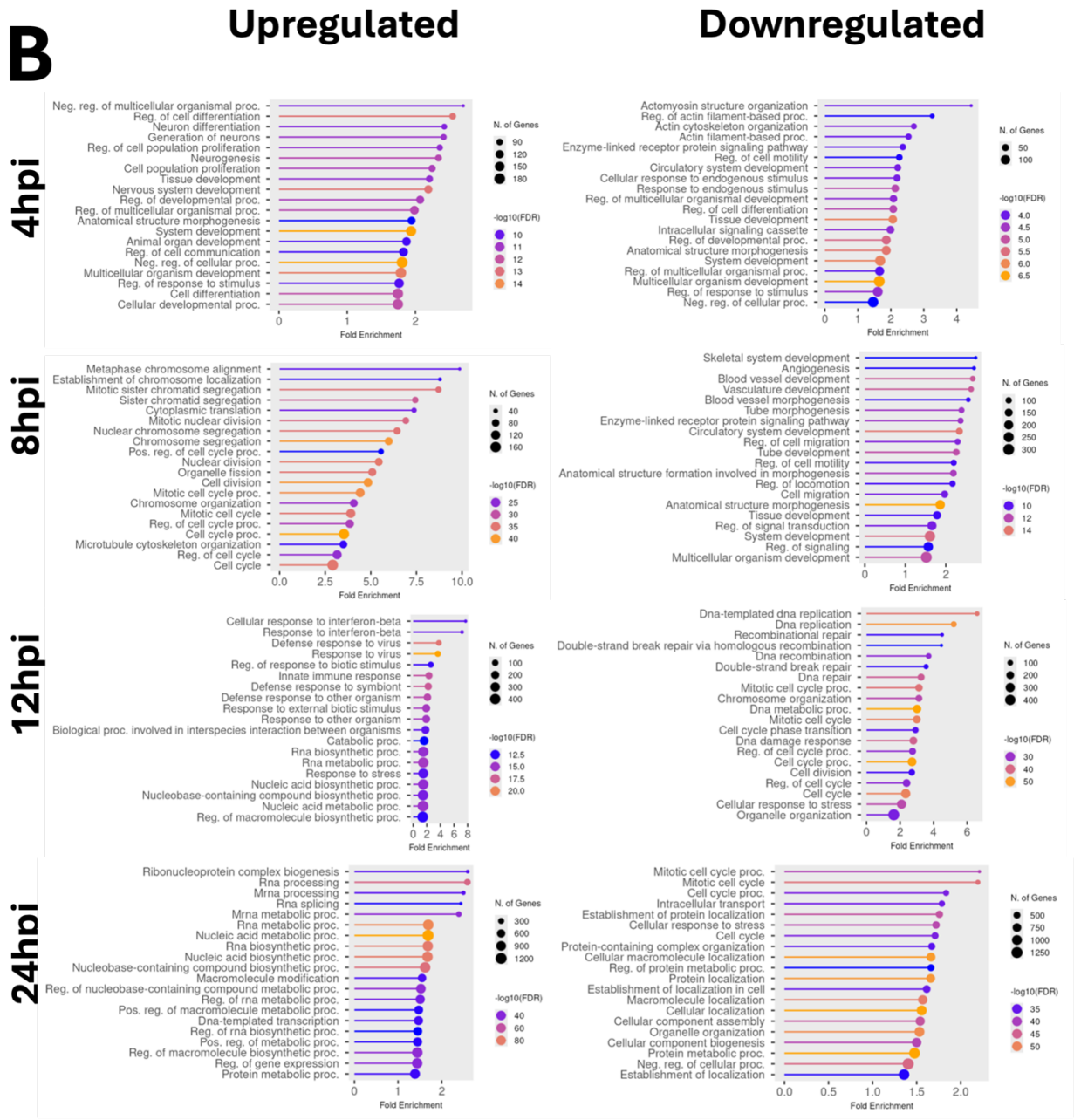

Figure 5. Pathways are differentially regulated upon viral infection, and change over time. A) Enrichment for the KEGG database. **B)** Enrichment for GO: Biological Process database. Keys for FDR and pathway gene number are indicated to the right of each individual plot. Gene lists were filtered for the following criteria: adjusted p value of <0.05; log2 fold change of >|0.5|; baseMean of >30.

2.5 Metabolic Pathway Analysis

We were unable to identify highly upregulated metabolic pathways with an unbiased pathway analysis. However, even a small perturbation of metabolic genes could represent massive phenotypic changes. With this in mind, I filtered our dataset for only metabolism-related genes registered in KEGG's master metabolism pathway for mice, mmu01100. I took genes from this filtered set, further filtered them to meet not only a criteria of an adjusted p value of < 0.05 but also a log2fc of 0.5 or higher (representing a raw fold change of ~1.4), and entered the resulting gene list into ShinyGO for pathway analysis. This analysis allows us to determine the most differentially expressed genes among all metabolic genes, keeping in mind the goal of finding a metabolic pathway that may be a good target for treating γHV infection. It is, however, important to note that these methods are biased and therefore render the "fold enrichment" value meaningless. Only the relative enrichment of each module compared to one another is important.

At 4hpi, KEGG identifies the top 3 enriched pathways as thiamine metabolism, nucleotide metabolism, and biosynthesis of cofactors (**Fig 6A**). The top two pathways at 8hpi are the pentose phosphate pathway and starch and sucrose metabolism. At 12hpi, the top pathways again shift. KEGG reports that they are phosphate and phosphinate metabolism, pentose and glucuronidate interconversions, and carbon metabolism. Finally, at 24hpi, KEGG indicates that ubiquinone, fatty acid, and steroid biosynthesis are upregulated.

I further interrogated specific pathways on a gene-by-gene basis. At the 4hr timepoint, thiamine metabolism (module mmu00730) was upregulated. Looking into the individual genes in that KEGG module, it appears it is primarily the adenylate kinase (Ak) genes that are upregulated, especially Ak1 and Ak5 (**Fig 6B**). However, while Ak1 (and most other Aks) remains upregulated over time, Ak5 is gradually downregulated. In the starch and sucrose pathway (mmu00500), the two most upregulated genes at 8hpi are Gbe1, a glycogen branching enzyme, and Pygm, which frees glucose monomers from glycogen (**Fig 6C**). In the ubiquinone pathway, enriched at 24hpi, Nqo1 and Coq3 were the two genes most upregulated at this timepoint (**Fig 6D**). Nqo1 is a member of the NADPH dehydrogenase family that plays a role in reducing redox stress by reducing quinones to hydroquinones[95]. Interestingly, Coq7 and Vkorc were

downregulated only at this timepoint. The remaining pathways enriched at 24hpi, steroid and fatty acid synthesis, reveal that Sc5d and Acsbg1, respectively, are the most upregulated at the relevant timepoint (**Figs 6E,F**). Scd5 converts lathosterol to 7-dehydrocholesterol, a precursor for vitamin D, while Acsbg1 is thought to catalyze the addition of CoA specifically to long-chain fatty acids[96].

Although glycolysis specifically was not indicated to be upregulated by our data, previous metabolomic work indicates that certain intermediates in the pathway are upregulated[54]. Hif1a, which senses ambient oxygen and induces glycolysis[97-99], also had targets enriched in my transcription factor network analysis at 4hpi. I therefore decided to look at individual genes in the pathway for further scrutiny (**Fig 6G**). This analysis revealed that Hk2, but not Hk1, is upregulated at 4hpi. Eno2, an isoform of phosphopyruvate hydratase, is upregulated at 12 and 24hpi, whereas another isoform, Eno3, is downregulated at all timepoints. Hif1a is slightly but significantly upregulated at 4hpi, and substantially downregulated at 12 and 24hpi.

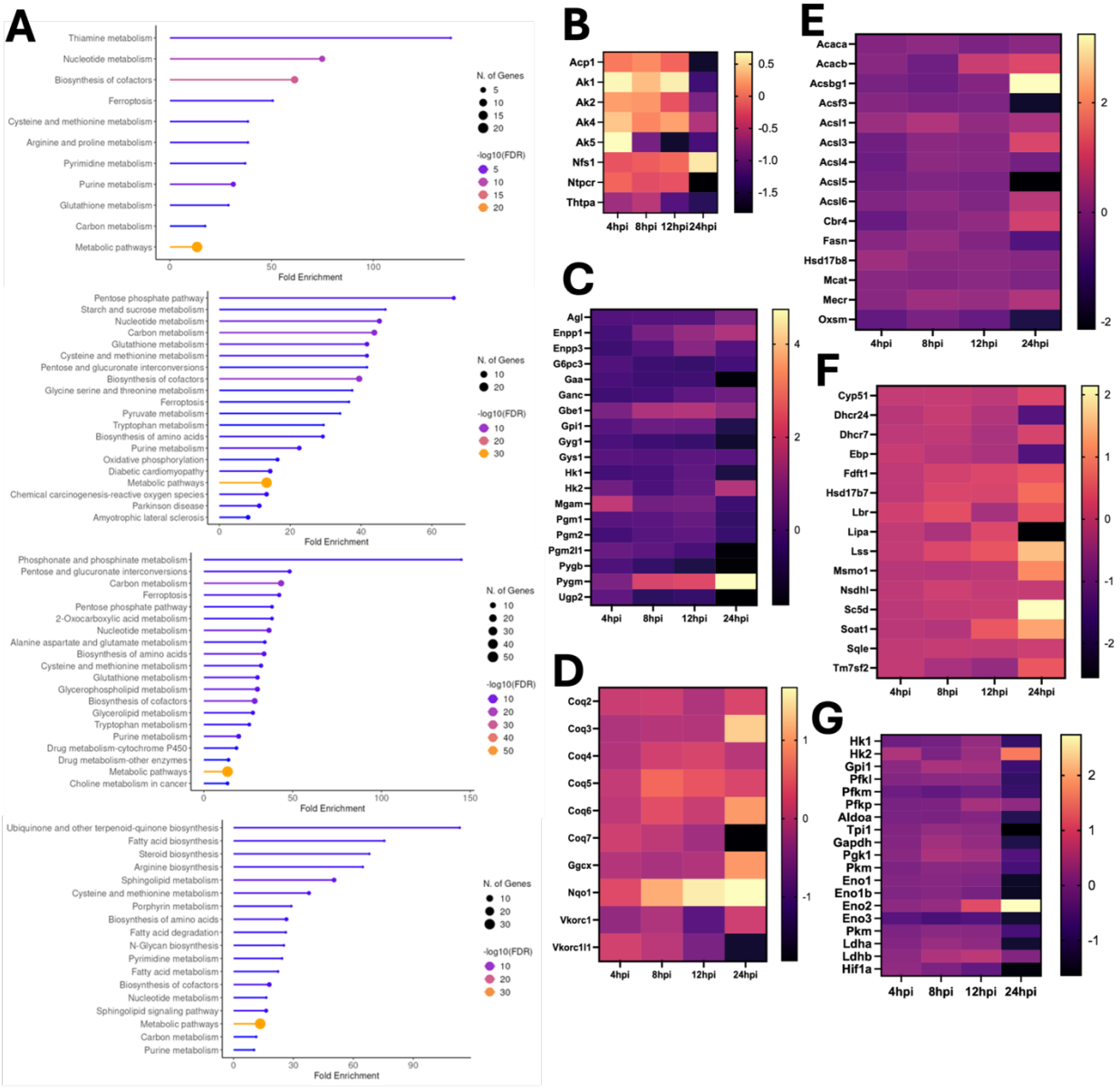

Figure 6. Top metabolic pathways expressed during MHV-68 infection. A) KEGG enrichment for top upregulated pathways at 4, 8, 12, and 24hpi following selection of genes in the pathway mmu01100, the master metabolic pathway. Keys for FDR and pathway gene number are indicated to the right of each individual plot. Gene lists were filtered for the following criteria: adjusted p value of <0.05; log2 fold change of >0.5; baseMean of >30.**B)** heatmap of genes in the thiamine metabolism pathway (mmu00730) over time. **C)** heatmap of genes in the starch and sucrose pathway (mmu00500) over time. **D)** heatmap of genes in the ubiquinone and other terpenoid-quinone biosynthesis pathway (mmu00130) over time. **E)** heatmap of genes in the fatty acid synthesis pathway (mmu00061) over time. **F)** heatmap of genes in the

steroid synthesis (mmu00100) pathway over time. **G)** heatmap of genes in the glycolysis pathway over time.

2.6 Evidence for Redox Stress

Oxidative phosphorylation was the most downregulated pathway at 24hpi (**Fig 5A**) even as the quinones COX1 and COX2 were among the most upregulated transcripts at 24hpi (**Fig 3B**). In addition, glutathione and ferroptosis pathways were enriched in most timepoints, though they were not among the most enriched. This prompted us to look further into metabolic pathways that might be modulating redox stress.

Transcripts encoding electron transport chain complex proteins became gradually more upregulated over time (**Fig 7A**). However, this was only true for mitochondrial complex members, not genes encoded by the nuclear compartment. Complex II, which has no mitochondrial components, was not upregulated. This is in contrast to the unbiased pathway analysis of genes significantly DE at 24hpi, which showed a downregulation of oxidative phosphorylation. It is important to mention that the GO:BP pathway contains regulatory genes in addition to the members that actually make up the Complexes I-V of the electron transport chain.

The pentose phosphate pathway (PPP) was among the top three upregulated pathways via KEGG annotation at 8hpi. The PPP is the primary source of NADPH, which primarily provides electrons for reduction power in the glutathione and fatty acid biosynthesis pathways, among other processes. Analysis of each gene in the pentose phosphate pathway shows that the enzymes that generate NADPH – G6pd2, G6pdx, and Pgd – are the most upregulated (**Fig 7B**). Interestingly, G6pd2, but not G6pdx (a paralog that shares the same function) is downregulated at 4hpi. Of note, G6pd is considered to be the rate-limiting step of the PPP. The main enzyme of the recycling part of this pathway – Tkt – is downregulated at 24hrpi.

There are several different arms of the ferroptosis pathway: iron storage, iron transport, arachidonic acid metabolism, glutathione metabolism, and mitochondrial-related genes. In clustering these genes together in the heatmap of their expression, it appears that certain members of the glutathione pathway are upregulated, but not all (**Fig 7C**). Additionally, while other members of the ferritin storage pathway are not particularly overexpressed, the ferritin light (Ftl) and heavy (Fth) chains are upregulated. Finally, the iron exporter Slc40a1 was upregulated.

While the ferroptosis pathway as recorded in KEGG subsumes a portion of the glutathione pathway, it does not contain all of it. I therefore also analyzed the entire glutathione pathway. The glutamate cysteine ligases, as well as glutamate synthetase, the enzymes that generate glutathione, were upregulated broadly upregulated across timepoints (**Fig 7D**). Additionally, Slc7a11, which imports cysteine that is necessary for glutathione synthesis, was also upregulated (**Fig 7E**).

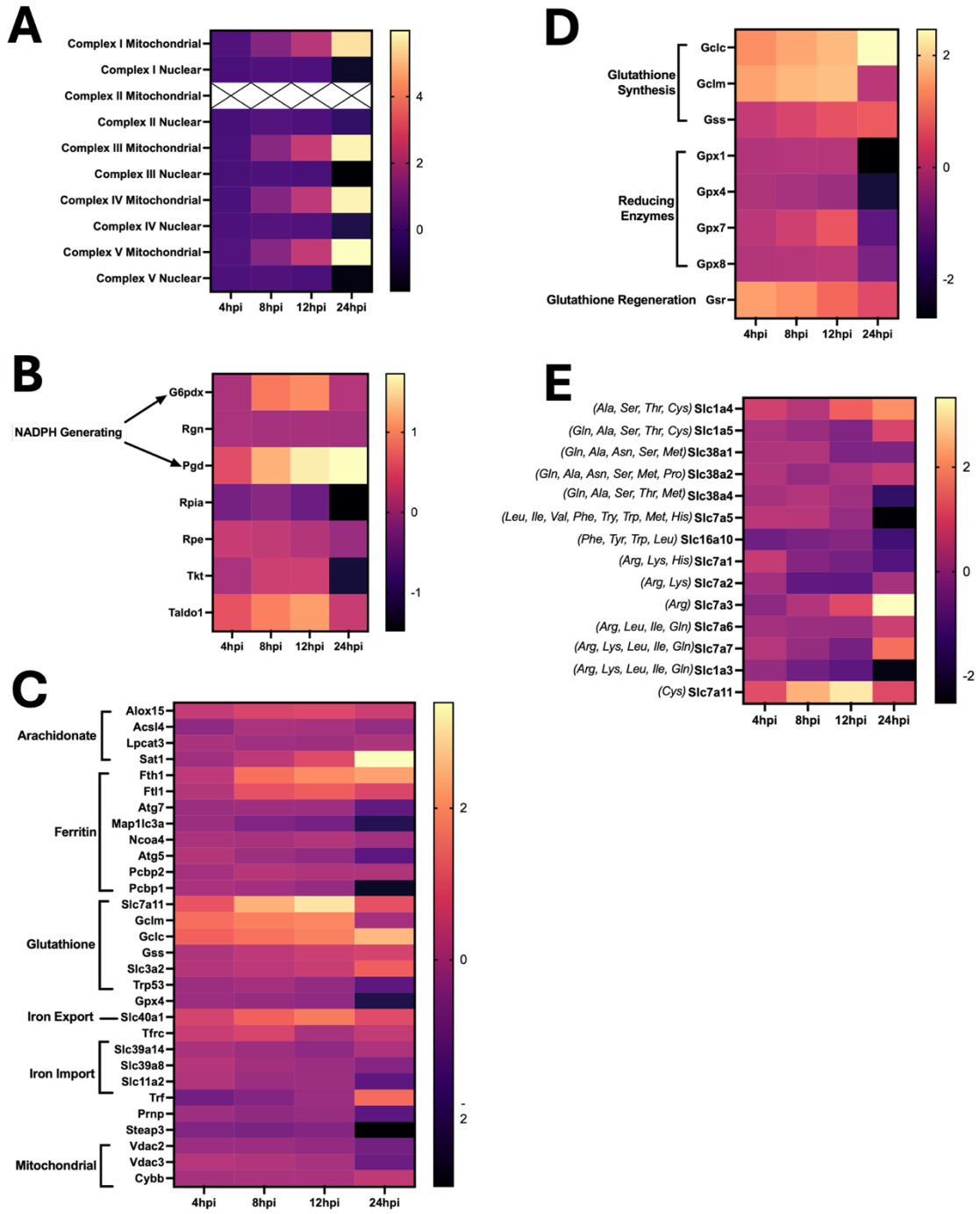

Figure 7. Pathways relating to redox stress are upregulated during MHV-68 infection of NIH3T3 cells. A) Heatmap for the pentose phosphate pathway, with enzymes that generate NADPH indicated. **B)** Heat map of the electron transport chain, with averaged expression of each transcript in each complex. Complexes are further divided into nuclear and mitochondrial encoded. **C)** Heatmap of genes in the ferroptosis pathway, with labels indicating which arm of the pathway each gene belongs to. **D)** Heatmap of enzymes involved in glutathione synthesis. **E)** Heatmap of amino acid transporters.

2.7 Epigenetic modifiers: Changes in Histone Lysine Methyltransferases and Demethylases

I began my analysis of chromatin dynamics during MHV-68 infection by investigating histone methylases and demethylases. Because each histone methyltransferase and demethylase acts independently of others and are not necessarily in the same pathway, I also made heatmaps to visualize the top differentially expressed Kmts (**Fig 8A**) and Kdms (**Fig 8B**). Notable Kdms include Kdm7a, which demethylates H3K9/27/36; it is the most downregulated gene in this group at 4hpi,but is gradually upregulated over time. Kdm2b is the most downregulated at 24hpi,and begins to be downregulated at 8hpi. Kdm5b, an H3K4 demethylase, is the most upregulated at 12hpi and maintains high expression at 24hpi. Among the Kmts, Suv39h1/2, Nsd2, and Ezh2 are notable for being downregulated at 12hpi. The Suv39hs catalyze methylation at H3K9, whereas Nsd2 methylates H3K36 and Ezh2 is the sole methylator of H3K27. Dot1L, which catalyzes the unusual methylation of H3K79, is very upregulated at 12hpi, whereas the H3K4 and H3K36-methylating Prdm9 is the most upregulated at 24hpi.

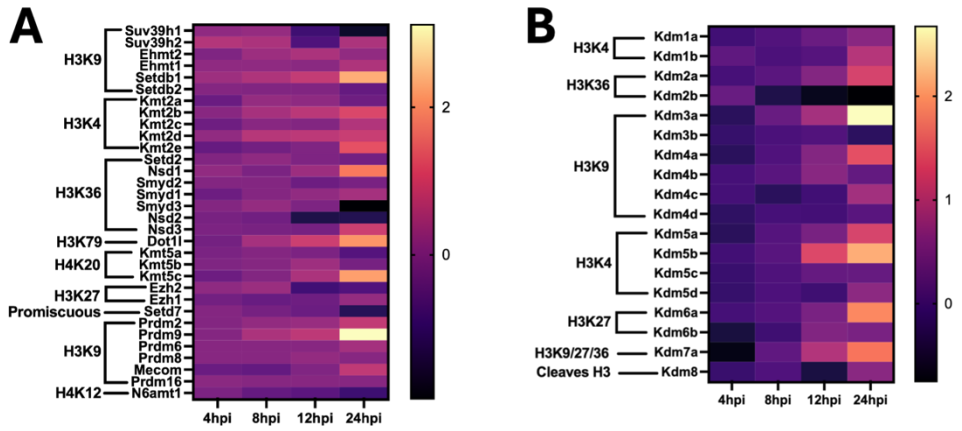

Figure 8. Differential expression of histone methylating (A) and demethylating (B) enzymes during MHV-68 infection in NIH3T3 cells.

2.8 Changes in Histone Variants and Histone Chaperones

Due to previous reports indicating that the histone variants H2AX and H2AZ are important for γHV proliferation, I also decided to look into histone variants. Most histone variants were either not expressed at all or expressed very few copies; I generated a heatmap that contains only the histone variants expressed at an average of 30 copies or more over all samples (**Fig 9A**). H2AX was most highly

expressed at 12hpi and, interestingly, was downregulated at 24hpi. One variant of, H2AZ, H2az1, was almost as highly expressed as H2AX. One locus that expresses canonical H2A, H2ac23, was very upregulated at 24hrpi. However, the most highly expressed histone variant from 4-12hpi was CENP-A, a centromeric variant of H3. Another intriguing result of this analysis was the downregulation of all expressed H1 variants starting at 12hpi, and especially H1.0 (H1f0) being very downregulated at 24hpi.

Finally, given the evident DE of histone variants at 24hpi, I assessed histone chaperones (**Fig 9B**). Caf1 complex proteins were downregulated starting at 12hpi, and maintained this downregulation through 24hpi. Interestingly, Asf1b, but not Asf1a, showed a similar pattern. In contrast, Daxx showed the opposite pattern – it was upregulated starting at 12hpi, into 24hpi.

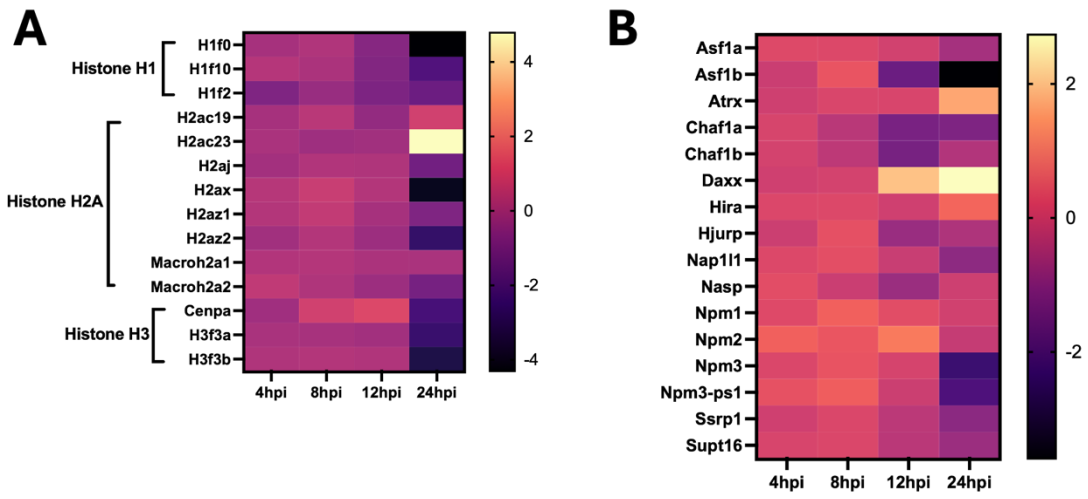

Figure 9. Figure 8. Differential expression of (A) histone transcripts and (B) histone chaperones during MHV-68 infection in NIH3T3 cells. Transcripts were filtered to meet a baseMean of >30.

2.9 Other Perturbations in Chromatin Biology

There are few annotated chromatin-related pathways in any of the major gene ontology databases; this is certainly true of the KEGG and GO databases. In an effort to expand the list of potential drug targets, I hand-curated a list of a variety of chromatin-related genes based on the existing literature[100-117]. This list

contains 258 genes and includes acetylating enzymes, deacetylating enzymes and associated complexes, PRC1 and PRC2 complex members, the BAF complex, and well-characterized readers/writers/erasers of certain H3 methylations.

At 4hpi, 3/10 of the top genes were related to PRC1, though the catalytic component of the complex (Ring1) was not significantly upregulated until 24hpi (**Fig 10A**). 3/10 of the top genes were also related to a variety of different deacetylases. The chromatin-related gene most highly expressed at this timepoint was Tet1, a DNA demethylase. At 8hpi, Tet1 is again the most highly expressed in this gene list; furthermore, 3/10 of the top genes are related to DNA methylation, including the Tet1-associated protein Gadd45a and also Tet2. 4/10 of the top transcripts at this timepoint are related to histone deacetylation. Again at 12hpi 4/10 of the top genes are related to DNA demethylation, including, again, Tet1 and Tet2, though Tet2 is now more highly expressed. 3/10 genes are related to histone deacetylation, and 2/10 are related to Polycomb complexes. At 24hpi, Tet2 is the most highly expressed gene in this list, though it is now the only DNA methylation-associated gene to make the top 10. 3/10 genes are related to Polycomb, and 3/10 are related to histone deacetylation. Sirt1, Sirt7, and Arid4b are also consistently among the top 10 across all timepoints.

Due to the early upregulation of Tet1 (4hpi) and the late upregulation of Tet2 (12&24hpi), we decided to test the effects of the Tet1/2 inhibitor Bobcat339 on viral proliferation. Bobcat339 reduced viral titer (normalized to cell count) by a factor of ~4 (**Fig 10C**).

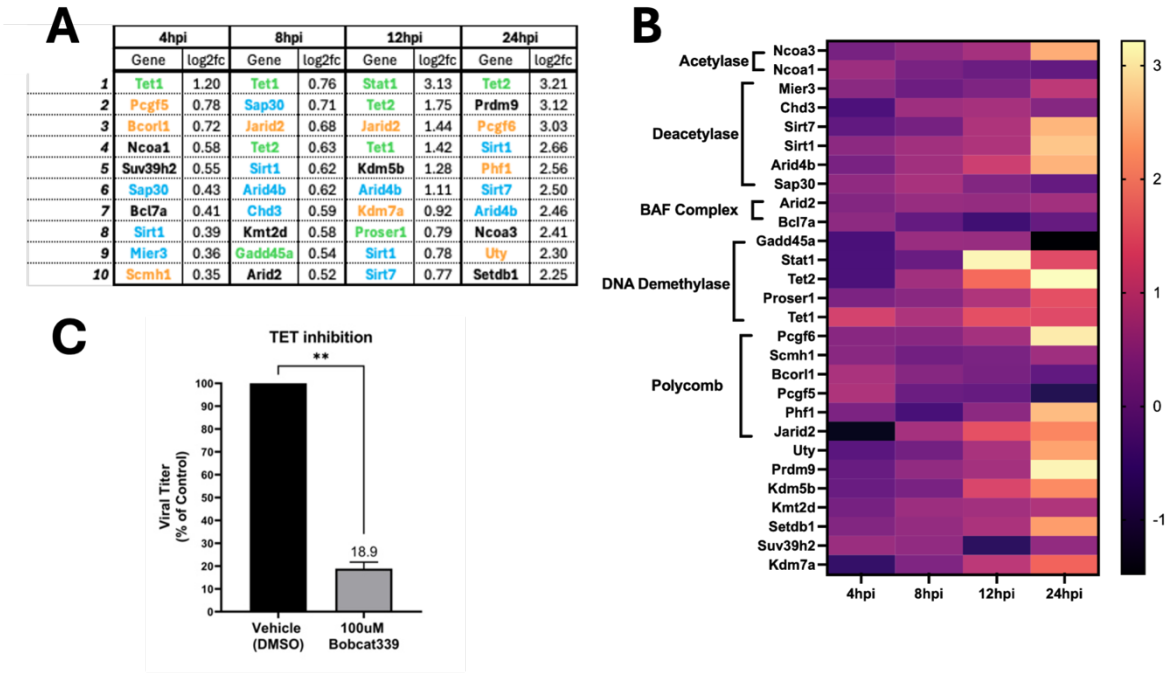

Figure 10. Top 10 expressed chromatin-related genes in each timepoint. A) list of top ten most upregulated chromatin-associated genes at each timepoint. **B)** heatmap following all genes identified in (A) over time. Genes are sorted and labelled by function. **C)** bar graph showing viral titers in NIH3T3 cells infected with MHV-68 with and without the Tet1/2 inhibitor Bobcat 339. Viral titer was normalized to cell count to account for potential host cell death.

3: IMPLICATIONS AND FUTURE DIRECTIONS

3.1 MHV-68 Recapitulates Many Aspects of Human γHV Metabolic Rearrangements

Previous reports indicate that the human γHVs EBV and KSHV instigate a variety of metabolic changes in their host cells. Notable perturbations include an increase in aerobic glycolysis and lactate production, otherwise known as the Warburg effect; an increase in fatty acid synthesis, with a concomitant increase in the PPP also noted; an increase in nucleotide production; and an increase in glutaminolysis[28,29]. Regarding glycolysis, we observed a mild increase in most glycolytic enzymes from 4-12hpi, with Hk2 and Eno2 upregulated throughout infection. Importantly, we also observed modest upregulation of lactate dehydrogenases Ldha and Ldhb, supporting the idea that MHV-68 induces the Warburg effect, especially given a previous report that lactate itself is upregulated[54]. Additionally, I observed an enrichment of Hif1a target genes at 4hpi (**Fig 4**). Hif1a is a transcription factor that is typically activated in response to hypoxia[97] and has been noted to be induced by KSHV and EBV[85-87]. Furthermore, the expression and stabilization of Hif1a is said to directly modulate upregulation in glycolysis in KSHV and EBV[98,99]. As MHV-68 induces both Hif1a and glycolytic gene expression, it stands to reason that Hif1a serves a similar role in inducing glycolysis during MHV-68 infection. However, full confirmation of the role of Hif1a in potentially inducing glycolysis during MHV-68 infection would require additional interrogation. For example, inhibition of Hif1a with one of the many available Hif1a inhibitors, followed by a measured reduction in glycolysis at the metabolomic, transcriptomic, and/or proteomic level would support this conclusion. It is also worth noting that Hif1a and many glycolytic intermediates (**Fig 6G**) are significantly downregulated at 24hrpi, which, when considered in conjunction with the gradual upregulation of ETC complex members, may indicate that MHV-68 shifts from sourcing energy primarily from the glycolysis + Warburg effect to sourcing energy from the ETC.

Glutaminolysis, the anaplerotic process in which glutamine is converted to alphaketoglutarate and enters the TCA cycle, has been noted to occur in herpesviral infections, including human γHV infection[28,29]. In human cytomegalovirus (HCMV), a betaherpesvirus, it has been documented that, while the carbon in glucose ends up in fatty acids[43], labeled glutamine enters the TCA cycle to replenish carbon[44].

Unfortunately, “glutaminolysis” is not a pathway registered under KEGG and thus it is impossible for an unbiased analysis to output it as a significant pathway. In examining the individual genes, however, there is evidence of mild, statistically significant upregulation of the enzymes involved in glutaminolysis, as well as glutamine transporters.

Pathway analysis also revealed that nucleotide metabolism was upregulated; it was the second most upregulated metabolic pathway at 4hr, the third at 8hr, and the seventh at 12hpi. Both purine and pyrimidine biosynthetic pathways were indicated to be upregulated at 4hpi, but by 8hpi purine biosynthesis was more enriched. This is in line with previous reports that purine metabolic intermediates are more enriched than pyrimidines in both EBV and KSHV[32,37,49], and also corroborates a previous report that MHV-68 induces the accumulation of more purine intermediates (such as xanthine and inosine) than pyrimidine intermediates (such as uridine and cytosine) at 8hpi[54].

The PPP is also considered to be integral to the *de novo* synthesis of nucleotides (purines especially, because it generated ribulose-5-phosphate), as well as being the primary source of cellular NADPH. This pathway was found to be the top most enriched metabolic pathway at 8hpi. Indeed, when looking into the individual genes within the PPP, the enzymes involved in generating NADPH are the most upregulated. This is supportive of the notion that the PPP may be upregulated in order to generate NADPH for FA synthesis. However, while fatty acid synthesis was identified as enriched at 24hpi, it was not identified as an enriched pathway at the same timepoint as the PPP (8hpi). Instead, another pathway was enriched at 8hpi that requires NADPH: glutathione related processes.

3.2 MHV-68 Infection of NIH3T3 Cells Induces Redox Stress

While the PPP and, specifically, NADPH producing enzymes were enriched at 8 and 12hpi, neither FA nor cholesterol synthesis were upregulated until 24hpi. However, glutathione related pathways were upregulated at 4, 8, and 12hpi. This suggests that the NADPH produced by the PPP may be acting as an electron donor to glutathione. Glutathione is the primary source of electrons for neutralizing cellular reactive oxygen species (ROS). It also did not escape my attention that COX1 and COX2, two members

of electron transport chain (ETC) Complex IV, are among the top two most upregulated transcripts at 24hpi. It is important to note here that the ETC is a major source of ROS[118], and aberrant upregulation of its processes is capable of changing the redox balance in a cell.

The extreme upregulation of these two genes prompted us to look into other members of the ETC, revealing a very clear gradual upregulation of ETC-related transcripts over time. Even more intriguing, when dividing ETC members into nuclear- vs mitochondrial-encoded, only the mitochondrial-encoded genes showed this gradual increase; this implies that MHV-68 uniquely manipulates mitochondrial gene expression, though the mechanism behind how it may achieve this is unclear. This is further supported by the downregulation of ubiquinone and other terpenoid quinones at 24hpi. The enzymes in this pathway are nuclear-encoded, and may represent an attempt by the host cell to downregulate an overactive ETC even while MHV-68 has artificially upregulated expression of mitochondrial ETC genes.

Ferroptosis is another metabolic pathway that was indicated to be enriched from 4 to 12hpi. Unlike many of the other metabolic pathways that only showed up upon filtering, ferroptosis is the second most enriched at 4hpi and the most enriched at 8hpi in my unbiased analysis. The key features of ferroptosis include its dependence on iron, the presence of fatty acid peroxidation, the downregulation of glutathione peroxidase Gpx4, and changes in mitochondrial structure[93]. Further investigation of this pathway revealed that there are multiple different groups of genes that modulate different subprocesses: arachidonic acid production, iron transport and storage, and glutathione synthesis being most of interest. Of the genes in these modules, the genes involved in the glutathione pathway Gclm, Gclc, Gss, and Gpx4, as well as the ferritin genes Ftl1 and Fth1, are known to be negative regulators of ferroptosis[119].

Glutathione synthesis was the primary process differentially expressed within the broader ferroptosis pathway, with iron importers also showing moderate downregulation. Clear, groupwide up- or downregulation was not observed for the other sub pathways. Looking at individual genes within the ferroptosis pathway, Gpx4 is mildly downregulated until 24hpi, when it is massively downregulated, and indicator of ferroptosis. However, the ferritin light and heavy chains, which are negative regulators of

ferroptosis, remain upregulated from 8 to 24hpi. In addition, the iron exporter Slc40a1 is upregulated throughout the course of infection. Other key markers of ferroptosis are, unfortunately, beyond the scope of this project. Validation that ferroptosis is occurring in this context may therefore include visualization of potential changes in mitochondrial structure during infection and measuring the accumulation of lipid peroxides and other ROS. There are commercially available dyes to visualize the presence of ROS using flow cytometry or microscopy.

Altogether, this data suggests that glycolysis may be briefly upregulated at early timepoints before the infected cell shifts to oxidative phosphorylation for its energy needs. The ETC becomes so upregulated that it induces redox stress, prompting the cell to increase NADPH and glutathione production. The upregulation of glutathione synthesis, iron export, and ferritin, combined with the downregulated of ferroptosis negative regulator Gpx4, suggests that ferroptosis may be triggered as a result of the oxidative stress.

Other viruses have been noted to manipulate host ROS, often in ways that promote viral proliferation[141,142,143]. For example, treatment of virally infected cells with antioxidants has been noted to reduce viral proliferation, suggesting a direct role of ROS in promoting viral reproduction. My proposed model suggests that it is the upregulation of the ETC that is important for the virus's energy needs over time, and not necessarily ROS itself. Targeting the ETC notoriously is extremely toxic[120], so we decided not to proceed with inhibiting the ETC. There are drugs available that neutralize superoxide radicals generated by the ETC, such as MitoTempo[143], but it is unclear whether ROS themselves are beneficial or harmful to viral production. I thus next moved to an analysis of potentially druggable chromatin-related pathways.

3.3 Chromatin Factors Relating to DNA Damage, H2AX and DAXX, are Differentially Expressed Throughout Infection

Massive transcriptional changes occurred during the first 24 hours of MHV-68 infection. Because one layer of transcriptional control is epigenetic modifications such as histone PTMs and DNA methylation, I

reasoned that, if there were epigenetic factors that were upregulated during infection, those factors may have been hijacked by the virus to rewire transcription. We could therefore proceed to inhibition of that epigenetic factor during infection to test whether it is important for transcription of host genes necessary for viral replication.

In evaluating all the known histone lysine methyltransferases (Kmts) and demethylases (Kdms), I found that substantial changes in expression of these factors only occurred at 24hpi. Of course, this does not necessarily mean that the PTMs they modulate are not important over the course of infection; in order to truly measure whether or not the H-PTM profile is significantly changed in MHV-68 infection, H-PTMs must be measured directly via methods such as ChIP-seq, CUT&RUN, or mass spectrometry. That being beyond the scope of my project, I instead decided to expand my search to other chromatin-related proteins.

The histone variant H2A.X has been reported to be important for viral proliferation in γHVs in general[75,76,121,122], whereas the histone variant H2AZ has been linked to EBV specifically[77]. In KSHV, H2A.X has been indicated to interact with viral protein LANA to tether the episome to the host genome[76]; H2AZ appears to serve a similar role in EBV through its interaction with viral protein EBNA1[77].
Due to this pre-existing evidence for the importance of at least one histone variant, I analyzed expression of all known histone variants throughout infection. Of those that were expressed, there was a modest global upregulation from 4-12hpi, with not only H2A.X but also H2A.Z and CENPA (an H3 variant) being slightly overrepresented compared to other histone variants. At 24hpi, there is a global downregulation of most histone variants, with the exception of canonical H2A, which remains upregulated. H2AX and H2AZ are notably more downregulated than other variants. Given that H2AX and H2AZ are involved in tethering of the viral episome to host chromosomes, and H2AX has already been suggested to be important for latency, I propose that H2AX and/or H2AZ transcriptional repression during lytic infection may be part of a mechanism that represses latency. Further studies to validate this may include selective degradation of H2AX during MHV-68 infection, followed by evaluation of the population of cells in the lytic vs latent state. If the population is skewed towards latency when H2AX is degraded, this would support my hypothesis.

Upon confirmation of changes in histone variant expression, I decided to investigate expression of histone chaperones. In particular, I was interested in the histone chaperone FACT, which has been known to chaperone H2A.X, specifically[123]. There was a small but significant decrease in both complex members at 12 and 24hpi. While this supports the idea that H2A variants are important in the context of MHV-68, again, this only appears to become important at later timepoints in infection. More interestingly, DAXX, a chaperone involved in response to DNA damage[124], was highly upregulated at 12 and 24hpi. This is in contrast to many different DNA damage response pathways being downregulated at 12hpi. The role of DNA damage in γHV lytic infection requires further exploration.

3.4 The Sin3 HDAC Complex, TETs, and Polycomb Complexes are Upregulated Throughout Lytic Infection

In an attempt to find an epigenetic factor that might be shaping earlier transcriptional changes, I next made a list of all chromatin modifying enzymes and complexes I am currently aware of[100-117]. Unlike my evaluation of the Kmts and Kdms, this time I included any other proteins known to act in a complex with histone readers/ writers. I also included DNA methyltransferases and demethylases, histone acetylases/ deacetylases, and histone remodeling complexes such as the BAF complex. This analysis revealed that DNA demethylases, non-enzymatic members of histone deacetylase complexes, and non-enzymatic members of the PRC complexes began to be upregulated at 4hpi, with their upregulation gradually increasing over infection.

It's important to note that Tet1/2 and Sin3, a major member of the Sin3 HDAC complex, have previously been described to interact[125,126]. Specifically, this interaction has been indicated to occur in embryonic stem cells and is involved in the de-repression of pluripotency-associated genes. While Sin3 itself was not among the top 10 most highly expressed chromatin factors, two other canonical members of the Sin3 complex, Arid4a and Sap30, were. EBV has previously been reported to induce expression of Tet1 and Tet2[127,128] , whereas in KSHV+ tumors Tet2 was noted to be transcriptionally upregulated[129]. Additionally, it has been found that, in KSHV, members of the Sin3 complex are not only present on viral chromatin in latency, but also directly recruit HDACs 1&2[130-132].

With evidence that Tet1/2 may also be important in the pathogenesis of the human γHVs, we decided to test the effects of the Tet2 inhibitor Bobcat339 on viral titers in MHV-68 infection of NIH3T3 cells. To our excitement, the drug inhibited viral production relative to cell proliferation by around fourfold, making it a promising potential candidate for further study. Next steps for determining the efficacy and safety of this drug for γHV treatment include further studies elucidating the mechanism behind why Tet1/2 function is important for viral reproduction. For example, the targets of Tet1/2 in this context are unknown and may be elucidated by bipartite sequencing to detect DNA methylation in conditions with and without viral infection, and with and without Bobcat339 treatment.

3.5 Summary

MHV-68 is genetically similar to the human γHVs KSHV and EBV. My data has supported the notion that it shares other notable similarities to the human γHVs, and is thus upheld as a robust model system for interrogating EBV and KSHV pathogenesis. At the transcriptional level, MHV-68 recapitulates key metabolic features of the human γHVs, including induction of the Warburg effect, evidence for glutaminolysis, and evidence for fatty acid synthesis at late timepoints. Additionally, my work indicated that Hif1a, also noted to be upregulated in EBV and KSHV[85-87,98,99] is induced at an early timepoint. Finally, while Tet1/2 and members of various HDAC complexes have been noted to be important for KSHV and EBV replication[127-132], to my knowledge, this is the first time they have been postulated to potentially work together in the context of viral infection.

We were also able to identify transcriptional evidence that MHV-68 infection induces redox stress, likely due to the upregulation of the ETC generating aberrant ROS. Confirmation of these processes occurring via the use of other methodologies is necessary, however. For example, the detection of lipid peroxidation, a hallmark of iron-mediated ferroptosis, can be quantified by the use of lipid peroxide labeling reagents. The same strategy can be used to detect other ROS, and may therefore be used to distinguish the primary source of electrons causing redox stress between iron release and ETC hyperactivity.

Finally, we were able to identify a potential drug target: Tet1/2. Inhibiting Tet1/2 with Bobcat339 reduced viral titers relative to cell proliferation. However, further work is needed to determine if the drug is efficacious *in vivo* and to determine the mechanism behind how Tet1/2 activity allows for maximal viral reproduction.

MATERIALS AND METHODS

Cell lines and reagents. NIH 3T3 cells (ATCC no. CRL-1658) or Vero cells (ATCC no. CCL-81) were cultured at 37°C and 5% CO_2 in complete Dulbecco's Modified Eagle Medium (DMEM) containing high glucose, L-glutamine, sodium pyruvate (Genesee no. 25-500), 1% penicillin streptomycin (Genesee no. 25-512), and 10% serum. NIH 3T3 cells were supplemented with 10% newborn calf serum (Fisher #16010159) and Vero cells were supplemented with 10% fetal bovine serum (Genesee no. 25-550). Drug stocks of 6-Aminonicotinamide (6-AN) (Fisher no. AAL0669203) and Bobcat339 hydrochloride (Selleckchem no. S6682) were dissolved in dimethyl sulfoxide (DMSO) and stored at -80°C.

Viruses and infection. MHV-68 viral stocks (ATCC no. VR-1465) were propagated via infection of NIH 3T3 cells or Vero cells at an MOI of 0.01-0.05. When ~80% of the cells detached, the cells and viral supernatant were freeze-thawed at -80°C and 37°C and then pelleted at 3,000 rpm for 10 min at 4°C. The cleared viral supernatant was centrifuged at 20,000 x g at 4°C for 90 minutes. The viral pellet was washed and then resuspended in serum-free (SF) DMEM. NIH 3T3 cells were Mock- or MHV-68-infected in SF DMEM for 2 hrs for RNA-seq analysis (MOI of 5) and drug assays (MOI of 0.1). After infection, the media was aspirated and replaced with complete DMEM media.

Viral titers and plaque assays. Viral titers were quantified through traditional viral plaque assays. Vero cells were seeded in 12-well plates at 250,000 cells in 1mL complete DMEM media. The next day, viral supernatants were 10-fold serial diluted (10^0 - 10^5) in SF DMEM. Vero cells were infected with 200uL of each dilution (in duplicate wells) for 90 min. After infection, the wells were aspirated and overlaid with 1.5 mL of media per well containing DMEM-glucose-glutamine-pyruvate (Thermofisher no. 12800017), sodium bicarbonate (Sigma no. S5761), 10% FBS, 1% methylcellulose (Sigma no M0387), 1% penicillin streptomycin, and 2.5 µg/mL Amphotericin B (Thermofisher no. 15290026). One week after infection, cells were fixed in 1 mL of 10% formalin per well for 30 minutes before media was discarded. The fix cells were stained with 1% crystal violet (Sigma no. C0775) in 20% methanol, rinsed with tap water, and then air dried. Plaque forming units per mL (pfu/mL) were calculated from duplicate wells using the equation:
(dilution factor) x (1 / 0.2mL) x (average pfu) = pfu/mL

RNA isolation, library prep, and RNA-sequencing. NIH 3T3 cells were seeded at a density of 2.2 million cells in 10-cm dishes approximately 4 h prior to infection. NIH 3T3 cells were Mock or MHV-68-infected at a MOI of 5 for 2 h in 3.5mL of SF DMEM media at 37°C. After infection, the media was aspirated and replaced with 10mL complete DMEM. At 4, 8, 12, and 24 hpi, matching pairs of Mock- or MHV-68-infected cells were harvested. The media was aspirated from each dish, washed with 10mL PBS, trypsinzed, and then resuspended in complete DMEM. The cells were centrifuged for 5 min at 300 x g at 20°C and the media was aspirated. The cell pellets were stored at -80°C. Samples were harvested at each time point in three independent experiments. RNA isolation was performed using the RNeasy Mini Kit (Qiagen no. 74104), Qiashredder (Qiagen no. 79654), and DNAse (Qiagen no. 79254) according to the manufacturers specifications. RNA concentration and purity were quantified at 260 nm and 280 nm using the Thermofisher "NanoDrop One" instrument. RNA integrity was analyzed using the Agilent High Sensitivity RNA ScreenTape System (Agilent no. 5067-5579) and the Agilent 4200 TapeStation instrument. Approximately 500 ng of RNA was converted to cDNA and library preparation was performed using the Illumina Stranded mRNA Prep (Illumina No. 20040532). Each sample was barcoded with the Illumina X Index. The library DNA quality was assessed using the Agilent High Sensitivity D1000 ScreenTape Assay (Agilent no. 5067-5587) and the Agilent 4200 TapeStation instrument. The library DNA concentration was quantified using the Qubit dsDNA HS Assay Kit (Thermofisher no. Q32854) and Qubit 4 instrument according to the manufacturers instructions. All samples were pooled at equal fractions, loaded, and sequenced in the NextSeq 2000 P3 flow cell with up to 1.2B single reads (Illumina no. 20100989) and using the NextSeq 2000 sequencer according to the manufacturers instructions.

RNA-sequencing data analysis.

Fastq files were downloaded from Illumina's basespace storage platform. Illumina pre-trims adapter sequences, so trimming was omitted from our pipeline. We checked quality scores with fastqc[133]. Alignment was then carried out using the splice-aware aligner STAR[134]. We first used STAR to index the RefSeq-annotated mm39 from NCBI, and then aligned our data to the indexed reference genome. Quantification was then carried out using salmon[135]. Post-quantification with salmon, the data was loaded

into R. Deeptools[136] was used to generate a PCA plot of all samples, using batch as a confounder. Even with batch as a confounder, replicate D did not cluster as tightly as the other replicates, and was henceforth dropped from the analysis. DESeq2[137] was utilized for differential expression analysis across paired mock vs viral samples using local fit parameters, with lfcShrink applied to reduce high log-fold changes in transcripts with low expression.

Gene Ontology (GO) pathway analysis.

To generate unbiased pathway analyses for each timepoint, genes were filtered to meet the following criteria: adjusted p value of <0.05; a log2 fold change of >|0.5|; and a baseMean of >30. Genes were further subdivided into up- and downregulated groups before being plugged into ShinyGO 0.85.0[138]. Pathway analysis for metabolism-related genes was carried out with the same methodology, with additional filtering for only genes in the KEGG[139] pathway mmu01100.

Drug assays, cell number, and viability. NIH 3T3 cells were seeded at a density of 760,000 cells in 6-cm dishes approximately 4 hr prior to infection. NIH 3T3 cells were Mock- or MHV-68-infected (MOI of 0.1) for 2 hr in SF DMEM. Following infection, the media was aspirated and replaced with complete DMEM supplemented with either vehicle (DMSO control), 35 μM 6-AN, or 100 μM Bobcat339. At 48 hpi, cellular supernatants were cleared by centrifugation at 10,000 rpm and the resulting viral supernatant was frozen at -80°C for future plaque assay analysis. The remaining cell pellet was pooled with matching sample trypsinized cells, centrifuged at 125 x g, and the cellular pellet was resuspended in 500 μL complete DMEM. Cell number and viability was assessed using a trypan blue exclusion assay and the Biorad T-20 automated cell counter (Biorad no. 1450102). Briefly, 15 μL of cells and 15 μL of trypan blue (Gibco 15250-061) were mixed and 10 μL was loaded on each side of a dual chambered slide (Biorad no. 1450003). Total-cells, live-cells, and percent viability were calculated by the Biorad T-20 automated cell counter.

Statistical analysis and graphs.

All heatmaps were generated using GraphPad Prism, as was the bar graph showing the effect of Bobcat339.

REFERENCES

1. Lan, K., & Luo, M. H. (2017). Herpesviruses: epidemiology, pathogenesis, and interventions. *Virologica Sinica*, *32*(5), 347–348. https://doi.org/10.1007/s12250-017-4108-2
2. Cohen J. I. (2020). Herpesvirus latency. *The Journal of clinical investigation*, *130*(7), 3361–3369. https://doi.org/10.1172/JCI136225
3. Engels, E. A., Atkinson, J. O., Graubard, B. I., McQuillan, G. M., Gamache, C., Mbisa, G., Cohn, S., Whitby, D., & Goedert, J. J. (2007). Risk factors for human herpesvirus 8 infection among adults in the United States and evidence for sexual transmission. *The Journal of infectious diseases*, *196*(2), 199–207. https://doi.org/10.1086/518791
4. Pellett, P. E., Wright, D. J., Engels, E. A., Ablashi, D. V., Dollard, S. C., Forghani, B., Glynn, S. A., Goedert, J. J., Jenkins, F. J., Lee, T. H., Neipel, F., Todd, D. S., Whitby, D., Nemo, G. J., Busch, M. P., & Retrovirus Epidemiology Donor Study (2003). Multicenter comparison of serologic assays and estimation of human herpesvirus 8 seroprevalence among US blood donors. *Transfusion*, *43*(9), 1260–1268. https://doi.org/10.1046/j.1537-2995.2003.00490.x
5. Qu, L., Jenkins, F., & Triulzi, D. J. (2010). Human herpesvirus 8 genomes and seroprevalence in United States blood donors. *Transfusion*, *50*(5), 1050–1056. https://doi.org/10.1111/j.1537-2995.2009.02559.x
6. Goncalves, P. H., Ziegelbauer, J., Uldrick, T. S., & Yarchoan, R. (2017). Kaposi sarcoma herpesvirus-associated cancers and related diseases. *Current opinion in HIV and AIDS*, *12*(1), 47–56. https://doi.org/10.1097/COH.0000000000000330
7. Longnecker, R., & Neipel, F. (2007). Introduction to the human γ-herpesviruses. In A. Arvin (Eds.) et. al., *Human Herpesviruses: Biology, Therapy, and Immunoprophylaxis*. Cambridge University Press.
8. Dunmire, S. K., Verghese, P. S., & Balfour, H. H., Jr (2018). Primary Epstein-Barr virus infection. *Journal of clinical virology : the official publication of the Pan American Society for Clinical Virology*, *102*, 84–92. https://doi.org/10.1016/j.jcv.2018.03.001
9. Bjornevik, K., Cortese, M., Healy, B. C., Kuhle, J., Mina, M. J., Leng, Y., Elledge, S. J., Niebuhr, D. W., Scher, A. I., Munger, K. L., & Ascherio, A. (2022). Longitudinal analysis reveals high prevalence of Epstein-Barr virus associated with multiple sclerosis. *Science (New York, N.Y.)*, *375*(6578), 296–301. https://doi.org/10.1126/science.abj8222
10. Debuysschere, C., Nekoua, M. P., & Hober, D. (2023). Markers of Epstein-Barr Virus Infection in Patients with Multiple Sclerosis. *Microorganisms*, *11*(5), 1262. https://doi.org/10.3390/microorganisms11051262
11. Azab, W., Dayaram, A., Greenwood, A. D., & Osterrieder, N. (2018). How Host Specific Are Herpesviruses? Lessons from Herpesviruses Infecting Wild and Endangered Mammals. *Annual review of virology*, *5*(1), 53–68. https://doi.org/10.1146/annurev-virology-092917-043227
12. Virgin, H. W., 4th, Latreille, P., Wamsley, P., Hallsworth, K., Weck, K. E., Dal Canto, A. J., & Speck, S. H. (1997). Complete sequence and genomic analysis of murine gammaherpesvirus 68. *Journal of virology*, *71*(8), 5894–5904. https://doi.org/10.1128/JVI.71.8.5894-5904.1997
13. Weed, D. J., & Damania, B. (2019). Pathogenesis of Human Gammaherpesviruses: Recent Advances. *Current clinical microbiology reports*, *6*(3), 166–174. https://doi.org/10.1007/s40588-019-00127-2
14. Weck, K. E., Kim, S. S., Virgin HW, I. V., & Speck, S. H. (1999). Macrophages are the major reservoir of latent murine gammaherpesvirus 68 in peritoneal cells. *Journal of virology*, *73*(4), 3273–3283. https://doi.org/10.1128/JVI.73.4.3273-3283.1999
15. Sunil-Chandra, N. P., Efstathiou, S., & Nash, A. A. (1992). Murine gammaherpesvirus 68 establishes a latent infection in mouse B lymphocytes in vivo. *The Journal of general virology*, *73 (Pt 12)*, 3275–3279. https://doi.org/10.1099/0022-1317-73-12-3275
16. Flaño, E., Husain, S. M., Sample, J. T., Woodland, D. L., & Blackman, M. A. (2000). Latent murine gamma-herpesvirus infection is established in activated B cells, dendritic cells, and macrophages. *Journal of immunology (Baltimore, Md. : 1950)*, *165*(2), 1074–1081. https://doi.org/10.4049/jimmunol.165.2.1074

17. Stewart, J. P., Usherwood, E. J., Ross, A., Dyson, H., & Nash, T. (1998). Lung epithelial cells are a major site of murine gammaherpesvirus persistence. *The Journal of experimental medicine*, *187*(12), 1941–1951. https://doi.org/10.1084/jem.187.12.1941

18. Damania, B., Kenney, S. C., & Raab-Traub, N. (2022). Epstein-Barr virus: Biology and clinical disease. *Cell*, *185*(20), 3652–3670. https://doi.org/10.1016/j.cell.2022.08.026

19. Raghu, H., Sharma-Walia, N., Veettil, M. V., Sadagopan, S., & Chandran, B. (2009). Kaposi's sarcoma-associated herpesvirus utilizes an actin polymerization-dependent macropinocytic pathway to enter human dermal microvascular endothelial and human umbilical vein endothelial cells. *Journal of virology*, *83*(10), 4895–4911. https://doi.org/10.1128/JVI.02498-08

20. Peng, L., Ryazantsev, S., Sun, R., & Zhou, Z. H. (2010). Three-dimensional visualization of gammaherpesvirus life cycle in host cells by electron tomography. *Structure (London, England : 1993)*, *18*(1), 47–58. https://doi.org/10.1016/j.str.2009.10.017

21. Zhu, S., & Viejo-Borbolla, A. (2021). Pathogenesis and virulence of herpes simplex virus. *Virulence*, *12*(1), 2670–2702. https://doi.org/10.1080/21505594.2021.1982373

22. Zhang, W., & Gao, S. J. (2012). Exploitation of Cellular Cytoskeletons and Signaling Pathways for Cell Entry by Kaposi's Sarcoma-Associated Herpesvirus and the Closely Related Rhesus Rhadinovirus. *Pathogens (Basel, Switzerland)*, *1*(2), 102–127. https://doi.org/10.3390/pathogens1020102

23. Gao, S. J., Deng, J. H., & Zhou, F. C. (2003). Productive lytic replication of a recombinant Kaposi's sarcoma-associated herpesvirus in efficient primary infection of primary human endothelial cells. *Journal of virology*, *77*(18), 9738–9749. https://doi.org/10.1128/jvi.77.18.9738-9749.2003

24. Kenney, S. C. (2007). Reactivation and lytic replication of EBV. In A. Arvin (Eds.) et. al., *Human Herpesviruses: Biology, Therapy, and Immunoprophylaxis*. Cambridge University Press.

25. De Clercq, E., & Li, G. (2016). Approved Antiviral Drugs over the Past 50 Years. *Clinical microbiology reviews*, *29*(3), 695–747. https://doi.org/10.1128/CMR.00102-15

26. Bubna A. K. (2015). Vorinostat-An Overview. *Indian journal of dermatology*, *60*(4), 419. https://doi.org/10.4103/0019-5154.160511

27. Jurado, A., Guo, H., & Schang, L. M. (2025). Epigenetic drugs against human DNA viruses and retroviruses. *Antiviral research*, *240*, 106218. https://doi.org/10.1016/j.antiviral.2025.106218

28. Sanchez, E. L., & Lagunoff, M. (2015). Viral activation of cellular metabolism. *Virology*, *479-480*, 609–618. https://doi.org/10.1016/j.virol.2015.02.038

29. Thaker, S. K., Ch'ng, J., & Christofk, H. R. (2019). Viral hijacking of cellular metabolism. *BMC biology*, *17*(1), 59. https://doi.org/10.1186/s12915-019-0678-9

30. Delgado, T., Sanchez, E. L., Camarda, R., & Lagunoff, M. (2012). Global metabolic profiling of infection by an oncogenic virus: KSHV induces and requires lipogenesis for survival of latent infection. *PLoS pathogens*, *8*(8), e1002866. https://doi.org/10.1371/journal.ppat.1002866

31. Sanchez, E. L., Pulliam, T. H., Dimaio, T. A., Thalhofer, A. B., Delgado, T., & Lagunoff, M. (2017). Glycolysis, Glutaminolysis, and Fatty Acid Synthesis Are Required for Distinct Stages of Kaposi's Sarcoma-Associated Herpesvirus Lytic Replication. *Journal of virology*, *91*(10), e02237-16. https://doi.org/10.1128/JVI.02237-16

32. Alfaez, A., Christopher, M. W., Garrett, T. J., & Papp, B. (2025). Analysis of Metabolomic Reprogramming Induced by Infection with Kaposi's Sarcoma-Associated Herpesvirus Using Untargeted Metabolomic Profiling. *International journal of molecular sciences*, *26*(7), 3109. https://doi.org/10.3390/ijms26073109

33. Zhu, Y., Ramos da Silva, S., He, M., Liang, Q., Lu, C., Feng, P., Jung, J. U., & Gao, S. J. (2016). An Oncogenic Virus Promotes Cell Survival and Cellular Transformation by Suppressing Glycolysis. *PLoS pathogens*, *12*(5), e1005648. https://doi.org/10.1371/journal.ppat.1005648

34. Zhu, Y., Li, T., Ramos da Silva, S., Lee, J. J., Lu, C., Eoh, H., Jung, J. U., & Gao, S. J. (2017). A Critical Role of Glutamine and Asparagine γ-Nitrogen in Nucleotide Biosynthesis in Cancer Cells Hijacked by an Oncogenic Virus. *mBio*, *8*(4), e01179-17. https://doi.org/10.1128/mBio.01179-17

35. Müller-Durovic, B., Jäger, J., Engelmann, C., Schuhmachers, P., Altermatt, S., Schlup, Y., Duthaler, U., Makowiec, C., Unterstab, G., Roffeis, S., Xhafa, E., Assmann, N., Trulsson, F.,

Steiner, R., Edwards-Hicks, J., West, J., Turner, L., Develioglu, L., Ivanek, R., Azzi, T., … Hess, C. (2024). A metabolic dependency of EBV can be targeted to hinder B cell transformation. *Science (New York, N.Y.)*, *385*(6704), eadk4898. https://doi.org/10.1126/science.adk4898

36. Wang, L. W., Wang, Z., Ersing, I., Nobre, L., Guo, R., Jiang, S., Trudeau, S., Zhao, B., Weekes, M. P., & Gewurz, B. E. (2019). Epstein-Barr virus subverts mevalonate and fatty acid pathways to promote infected B-cell proliferation and survival. *PLoS pathogens*, *15*(9), e1008030. https://doi.org/10.1371/journal.ppat.1008030

37. Wang, L. W., Shen, H., Nobre, L., Ersing, I., Paulo, J. A., Trudeau, S., Wang, Z., Smith, N. A., Ma, Y., Reinstadler, B., Nomburg, J., Sommermann, T., Cahir-McFarland, E., Gygi, S. P., Mootha, V. K., Weekes, M. P., & Gewurz, B. E. (2019). Epstein-Barr-Virus-Induced One-Carbon Metabolism Drives B Cell Transformation. *Cell metabolism*, *30*(3), 539–555.e11. https://doi.org/10.1016/j.cmet.2019.06.003

38. Delgado, T., Carroll, P. A., Punjabi, A. S., Margineantu, D., Hockenbery, D. M., & Lagunoff, M. (2010). Induction of the Warburg effect by Kaposi's sarcoma herpesvirus is required for the maintenance of latently infected endothelial cells. *Proceedings of the National Academy of Sciences of the United States of America*, *107*(23), 10696–10701. https://doi.org/10.1073/pnas.1004882107

39. Darekar, S., Georgiou, K., Yurchenko, M., Yenamandra, S. P., Chachami, G., Simos, G., Klein, G., & Kashuba, E. (2012). Epstein-Barr virus immortalization of human B-cells leads to stabilization of hypoxia-induced factor 1 alpha, congruent with the Warburg effect. *PloS one*, *7*(7), e42072. https://doi.org/10.1371/journal.pone.0042072

40. Heawchaiyaphum, C., Yoshiyama, H., Iizasa, H., Burassakarn, A., Tumurgan, Z., Ekalaksananan, T., & Pientong, C. (2023). Epstein-Barr Virus Promotes Oral Squamous Cell Carcinoma Stemness through the Warburg Effect. *International journal of molecular sciences*, *24*(18), 14072. https://doi.org/10.3390/ijms241814072

41. Bottero, V., Chakraborty, S., & Chandran, B. (2013). Reactive oxygen species are induced by Kaposi's sarcoma-associated herpesvirus early during primary infection of endothelial cells to promote virus entry. *Journal of virology*, *87*(3), 1733–1749. https://doi.org/10.1128/JVI.02958-12

42. Li, X., Feng, J., & Sun, R. (2011). Oxidative stress induces reactivation of Kaposi's sarcoma-associated herpesvirus and death of primary effusion lymphoma cells. *Journal of virology*, *85*(2), 715–724. https://doi.org/10.1128/JVI.01742-10

43. Vastag, L., Koyuncu, E., Grady, S. L., Shenk, T. E., & Rabinowitz, J. D. (2011). Divergent effects of human cytomegalovirus and herpes simplex virus-1 on cellular metabolism. *PLoS pathogens*, *7*(7), e1002124. https://doi.org/10.1371/journal.ppat.1002124

44. Chambers, J. W., Maguire, T. G., & Alwine, J. C. (2010). Glutamine metabolism is essential for human cytomegalovirus infection. *Journal of virology*, *84*(4), 1867–1873. https://doi.org/10.1128/JVI.02123-09

45. Liu, X., Zhu, C., Wang, Y., Wei, F., & Cai, Q. (2021). KSHV Reprogramming of Host Energy Metabolism for Pathogenesis. *Frontiers in cellular and infection microbiology*, *11*, 621156. https://doi.org/10.3389/fcimb.2021.621156

46. Lo, A. K., Lo, K. W., Ko, C. W., Young, L. S., & Dawson, C. W. (2013). Inhibition of the LKB1-AMPK pathway by the Epstein-Barr virus-encoded LMP1 promotes proliferation and transformation of human nasopharyngeal epithelial cells. *The Journal of pathology*, *230*(3), 336–346. https://doi.org/10.1002/path.4201

47. Lu, J., Tang, M., Li, H., Xu, Z., Weng, X., Li, J., Yu, X., Zhao, L., Liu, H., Hu, Y., Tan, Z., Yang, L., Zhong, M., Zhou, J., Fan, J., Bode, A. M., Yi, W., Gao, J., Sun, L., & Cao, Y. (2016). EBV-LMP1 suppresses the DNA damage response through DNA-PK/AMPK signaling to promote radioresistance in nasopharyngeal carcinoma. *Cancer letters*, *380*(1), 191–200. https://doi.org/10.1016/j.canlet.2016.05.032

48. Luo, G. G., & Ou, J. H. (2015). Oncogenic viruses and cancer. *Virologica Sinica*, *30*(2), 83–84. https://doi.org/10.1007/s12250-015-3599-y

49. Lamontagne, R. J., Soldan, S. S., Su, C., Wiedmer, A., Won, K. J., Lu, F., Goldman, A. R., Wickramasinghe, J., Tang, H. Y., Speicher, D. W., Showe, L., Kossenkov, A. V., & Lieberman, P. M. (2021). A multi-omics approach to Epstein-Barr virus immortalization of B-cells reveals

EBNA1 chromatin pioneering activities targeting nucleotide metabolism. *PLoS pathogens*, *17*(1), e1009208. https://doi.org/10.1371/journal.ppat.1009208

50. Yu, Y., Maguire, T. G., & Alwine, J. C. (2012). Human cytomegalovirus infection induces adipocyte-like lipogenesis through activation of sterol regulatory element binding protein 1. *Journal of virology*, *86*(6), 2942–2949. https://doi.org/10.1128/JVI.06467-11

51. Wudiri, G. A., & Nicola, A. V. (2017). Cellular Cholesterol Facilitates the Postentry Replication Cycle of Herpes Simplex Virus 1. *Journal of virology*, *91*(14), e00445-17. https://doi.org/10.1128/JVI.00445-17

52. Albano, C., Trifirò, L., Hewelt-Belka, W., Cairns, D. M., Pasquero, S., Griffante, G., Gugliesi, F., Bajetto, G., Garwolińska, D., Rossi, M., Vallino, M., Malerba, M., De Andrea, M., Kaplan, D. L., Dell'Oste, V., & Biolatti, M. (2025). The impact of fatty acid synthase on HSV-1 infection dynamics. *PLoS pathogens*, *21*(5), e1013068. https://doi.org/10.1371/journal.ppat.1013068

53. Farías, M. A., Cancino, F. A., Navarro, A. J., Duarte, L. F., Soto, A. A., Tognarelli, E. I., Ramm, M. J., Alarcón-Zapata, B. N., Cordero, J., San Martín, S., Agurto-Muñoz, C., Retamal-Díaz, A., Riedel, C. A., Barrera, N. P., Bustamante, L., Bueno, S. M., Kalergis, A. M., & González, P. A. (2025). HSV-1 alters lipid metabolism and induces lipid droplet accumulation in functionally impaired mouse dendritic cells. *iScience*, *28*(5), 112441. https://doi.org/10.1016/j.isci.2025.112441

54. Clark, S. A., Vazquez, A., Furiya, K., Splattstoesser, M. K., Bashmail, A. K., Schwartz, H., Russell, M., Bhark, S. J., Moreno, O. K., McGovern, M., Owsley, E. R., Nelson, T. A., Sanchez, E. L., & Delgado, T. (2023). Rewiring of the Host Cell Metabolome and Lipidome during Lytic Gammaherpesvirus Infection Is Essential for Infectious-Virus Production. *Journal of virology*, *97*(6), e0050623. https://doi.org/10.1128/jvi.00506-23

55. Piovesan, A., Pelleri, M. C., Antonaros, F., Strippoli, P., Caracausi, M., & Vitale, L. (2019). On the length, weight and GC content of the human genome. *BMC research notes*, *12*(1), 106. https://doi.org/10.1186/s13104-019-4137-z

56. Lammerding, J., Dahl, K. N., Discher, D. E., & Kamm, R. D. (2007). Nuclear mechanics and methods. *Methods in cell biology*, *83*, 269–294. https://doi.org/10.1016/S0091-679X(07)83011-1

57. Gkikopoulos, T., Havas, K. M., Dewar, H., & Owen-Hughes, T. (2009). SWI/SNF and Asf1p cooperate to displace histones during induction of the saccharomyces cerevisiae HO promoter. *Molecular and cellular biology*, *29*(15), 4057–4066. https://doi.org/10.1128/MCB.00400-09

58. Radman-Livaja, M., & Rando, O. J. (2010). Nucleosome positioning: how is it established, and why does it matter?. *Developmental biology*, *339*(2), 258–266. https://doi.org/10.1016/j.ydbio.2009.06.012

59. Kelso, T. W. R., Porter, D. K., Amaral, M. L., Shokhirev, M. N., Benner, C., & Hargreaves, D. C. (2017). Chromatin accessibility underlies synthetic lethality of SWI/SNF subunits in ARID1A-mutant cancers. *eLife*, *6*, e30506. https://doi.org/10.7554/eLife.30506

60. Schick, S., Grosche, S., Kohl, K. E., Drpic, D., Jaeger, M. G., Marella, N. C., Imrichova, H., Lin, J. G., Hofstätter, G., Schuster, M., Rendeiro, A. F., Koren, A., Petronczki, M., Bock, C., Müller, A. C., Winter, G. E., & Kubicek, S. (2021). Acute BAF perturbation causes immediate changes in chromatin accessibility. *Nature genetics*, *53*(3), 269–278. https://doi.org/10.1038/s41588-021-00777-3

61. Hodges, H. C., Stanton, B. Z., Cermakova, K., Chang, C. Y., Miller, E. L., Kirkland, J. G., Ku, W. L., Veverka, V., Zhao, K., & Crabtree, G. R. (2018). Dominant-negative SMARCA4 mutants alter the accessibility landscape of tissue-unrestricted enhancers. *Nature structural & molecular biology*, *25*(1), 61–72. https://doi.org/10.1038/s41594-017-0007-3

62. Iurlaro, M., Stadler, M. B., Masoni, F., Jagani, Z., Galli, G. G., & Schübeler, D. (2021). Mammalian SWI/SNF continuously restores local accessibility to chromatin. *Nature genetics*, *53*(3), 279–287. https://doi.org/10.1038/s41588-020-00768-w

63. Brahma, S., & Henikoff, S. (2024). The BAF chromatin remodeler synergizes with RNA polymerase II and transcription factors to evict nucleosomes. *Nature genetics*, *56*(1), 100–111. https://doi.org/10.1038/s41588-023-01603-8

64. Bracken, A. P., Brien, G. L., & Verrijzer, C. P. (2019). Dangerous liaisons: interplay between SWI/SNF, NuRD, and Polycomb in chromatin regulation and cancer. *Genes & development*, *33*(15-16), 936–959. https://doi.org/10.1101/gad.326066.119

65. Kadoch, C., Williams, R. T., Calarco, J. P., Miller, E. L., Weber, C. M., Braun, S. M., Pulice, J. L., Chory, E. J., & Crabtree, G. R. (2017). Dynamics of BAF-Polycomb complex opposition on heterochromatin in normal and oncogenic states. *Nature genetics*, *49*(2), 213–222. https://doi.org/10.1038/ng.3734

66. Machida, S., Takizawa, Y., Ishimaru, M., Sugita, Y., Sekine, S., Nakayama, J. I., Wolf, M., & Kurumizaka, H. (2018). Structural Basis of Heterochromatin Formation by Human HP1. *Molecular cell*, *69*(3), 385–397.e8. https://doi.org/10.1016/j.molcel.2017.12.011

67. Zeng, W., Ball, A. R., Jr, & Yokomori, K. (2010). HP1: heterochromatin binding proteins working the genome. *Epigenetics*, *5*(4), 287–292. https://doi.org/10.4161/epi.5.4.11683

68. Uckelmann, M., & Davidovich, C. (2024). Chromatin compaction by Polycomb group proteins revisited. *Current opinion in structural biology*, *86*, 102806. https://doi.org/10.1016/j.sbi.2024.102806

69. King, H. W., Fursova, N. A., Blackledge, N. P., & Klose, R. J. (2018). Polycomb repressive complex 1 shapes the nucleosome landscape but not accessibility at target genes. *Genome research*, *28*(10), 1494–1507. https://doi.org/10.1101/gr.237180.118

70. Zhao, J., Wang, M., Chang, L., Yu, J., Song, A., Liu, C., Huang, W., Zhang, T., Wu, X., Shen, X., Zhu, B., & Li, G. (2020). RYBP/YAF2-PRC1 complexes and histone H1-dependent chromatin compaction mediate propagation of H2AK119ub1 during cell division. *Nature cell biology*, *22*(4), 439–452. https://doi.org/10.1038/s41556-020-0484-1

71. Millán-Zambrano, G., Burton, A., Bannister, A. J., & Schneider, R. (2022). Histone post-translational modifications - cause and consequence of genome function. *Nature reviews. Genetics*, *23*(9), 563–580. https://doi.org/10.1038/s41576-022-00468-7

72. Zhang, T., Cooper, S., & Brockdorff, N. (2015). The interplay of histone modifications - writers that read. *EMBO reports*, *16*(11), 1467–1481. https://doi.org/10.15252/embr.201540945

73. Kuo, L. J., & Yang, L. X. (2008). Gamma-H2AX - a novel biomarker for DNA double-strand breaks. *In vivo (Athens, Greece)*, *22*(3), 305–309.

74. Kutluay, S. B., & Triezenberg, S. J. (2009). Role of chromatin during herpesvirus infections. *Biochimica et biophysica acta*, *1790*(6), 456–466. https://doi.org/10.1016/j.bbagen.2009.03.019

75. Jha, H. C., Upadhyay, S. K., A J Prasad, M., Lu, J., Cai, Q., Saha, A., & Robertson, E. S. (2013). H2AX phosphorylation is important for LANA-mediated Kaposi's sarcoma-associated herpesvirus episome persistence. *Journal of virology*, *87*(9), 5255–5269. https://doi.org/10.1128/JVI.03575-12

76. Tarakanova, V. L., Leung-Pineda, V., Hwang, S., Yang, C. W., Matatall, K., Basson, M., Sun, R., Piwnica-Worms, H., Sleckman, B. P., & Virgin, H. W., 4th (2007). Gamma-herpesvirus kinase actively initiates a DNA damage response by inducing phosphorylation of H2AX to foster viral replication. *Cell host & microbe*, *1*(4), 275–286. https://doi.org/10.1016/j.chom.2007.05.008

77. Castro-Muñoz, L. J., Maestri, D., Yoon, L., Karisetty, B. C., Tempera, I., & Lieberman, P. (2025). Histone variant H2A.Z cooperates with EBNA1 to maintain Epstein-Barr virus latent epigenome. *mBio*, *16*(8), e0030225. https://doi.org/10.1128/mbio.00302-25

78. Toth, Z., Maglinte, D. T., Lee, S. H., Lee, H. R., Wong, L. Y., Brulois, K. F., Lee, S., Buckley, J. D., Laird, P. W., Marquez, V. E., & Jung, J. U. (2010). Epigenetic analysis of KSHV latent and lytic genomes. *PLoS pathogens*, *6*(7), e1001013. https://doi.org/10.1371/journal.ppat.1001013

79. Günther, T., & Grundhoff, A. (2010). The epigenetic landscape of latent Kaposi sarcoma-associated herpesvirus genomes. *PLoS pathogens*, *6*(6), e1000935. https://doi.org/10.1371/journal.ppat.1000935

80. González-Almela, E., Castells-Garcia, A., Le Dily, F., Merino, M. F., Carnevali, D., Cusco, P., Di Croce, L., & Cosma, M. P. (2025). Herpes simplex virus type 1 reshapes host chromatin architecture via transcription machinery hijacking. *Nature communications*, *16*(1), 5313. https://doi.org/10.1038/s41467-025-60534-6

81. Hansen, K. D., Sabunciyan, S., Langmead, B., Nagy, N., Curley, R., Klein, G., Klein, E., Salamon, D., & Feinberg, A. P. (2014). Large-scale hypomethylated blocks associated with

Epstein-Barr virus-induced B-cell immortalization. *Genome research*, *24*(2), 177–184. https://doi.org/10.1101/gr.157743.113

82. Hernando, H., Shannon-Lowe, C., Islam, A. B., Al-Shahrour, F., Rodríguez-Ubreva, J., Rodríguez-Cortez, V. C., Javierre, B. M., Mangas, C., Fernández, A. F., Parra, M., Delecluse, H. J., Esteller, M., López-Granados, E., Fraga, M. F., López-Bigas, N., & Ballestar, E. (2013). The B cell transcription program mediates hypomethylation and overexpression of key genes in Epstein-Barr virus-associated proliferative conversion. *Genome biology*, *14*(1), R3. https://doi.org/10.1186/gb-2013-14-1-r3

83. Hernando, H., Islam, A. B., Rodríguez-Ubreva, J., Forné, I., Ciudad, L., Imhof, A., Shannon-Lowe, C., & Ballestar, E. (2014). Epstein-Barr virus-mediated transformation of B cells induces global chromatin changes independent to the acquisition of proliferation. *Nucleic acids research*, *42*(1), 249–263. https://doi.org/10.1093/nar/gkt886

84. Oh, J., & Fraser, N. W. (2008). Temporal association of the herpes simplex virus genome with histone proteins during a lytic infection. *Journal of virology*, *82*(7), 3530–3537. https://doi.org/10.1128/JVI.00586-07

85. Sung, W. W., Chu, Y. C., Chen, P. R., Liao, M. H., & Lee, J. W. (2016). Positive regulation of HIF-1A expression by EBV oncoprotein LMP1 in nasopharyngeal carcinoma cells. *Cancer letters*, *382*(1), 21–31. https://doi.org/10.1016/j.canlet.2016.08.021

86. Ma, T., Patel, H., Babapoor-Farrokhran, S., Franklin, R., Semenza, G. L., Sodhi, A., & Montaner, S. (2015). KSHV induces aerobic glycolysis and angiogenesis through HIF-1-dependent upregulation of pyruvate kinase 2 in Kaposi's sarcoma. *Angiogenesis*, *18*(4), 477–488. https://doi.org/10.1007/s10456-015-9475-4

87. Carroll, P. A., Kenerson, H. L., Yeung, R. S., & Lagunoff, M. (2006). Latent Kaposi's sarcoma-associated herpesvirus infection of endothelial cells activates hypoxia-induced factors. *Journal of virology*, *80*(21), 10802–10812. https://doi.org/10.1128/JVI.00673-06

88. Alzhanova, D., Meyo, J. O., Juarez, A., & Dittmer, D. P. (2021). The ORF45 Protein of Kaposi Sarcoma-Associated Herpesvirus Is an Inhibitor of p53 Signaling during Viral Reactivation. *Journal of virology*, *95*(23), e0145921. https://doi.org/10.1128/JVI.01459-21

89. Chatterjee, K., Das, P., Chattopadhyay, N. R., Mal, S., & Choudhuri, T. (2019). The interplay between Epstein-Bar virus (EBV) with the p53 and its homologs during EBV associated malignancies. *Heliyon*, *5*(11), e02624. https://doi.org/10.1016/j.heliyon.2019.e02624

90. Li, M., Gao, X., Su, Y., Shan, S., Qian, W., Zhang, Z., & Zhu, D. (2024). FOXM1 transcriptional regulation. *Biology of the cell*, *116*(9), e2400012. https://doi.org/10.1111/boc.202400012

91. Khan, M. A., Khan, P., Ahmad, A., Fatima, M., & Nasser, M. W. (2023). FOXM1: A small fox that makes more tracks for cancer progression and metastasis. *Seminars in cancer biology*, *92*, 1–15. https://doi.org/10.1016/j.semcancer.2023.03.007

92. Ito, T., Kohashi, K., Yamada, Y., Iwasaki, T., Maekawa, A., Kuda, M., Hoshina, D., Abe, R., Furue, M., & Oda, Y. (2016). Prognostic Significance of Forkhead Box M1 (FOXM1) Expression and Antitumor Effect of FOXM1 Inhibition in Angiosarcoma. *Journal of Cancer*, *7*(7), 823–830. https://doi.org/10.7150/jca.14461

93. Dixon, S. J., & Olzmann, J. A. (2024). The cell biology of ferroptosis. *Nature reviews. Molecular cell biology*, *25*(6), 424–442. https://doi.org/10.1038/s41580-024-00703-5

94. Wu, G., Fang, Y. Z., Yang, S., Lupton, J. R., & Turner, N. D. (2004). Glutathione metabolism and its implications for health. *The Journal of nutrition*, *134*(3), 489–492. https://doi.org/10.1093/jn/134.3.489

95. Ross, D., & Siegel, D. (2021). The diverse functionality of NQO1 and its roles in redox control. *Redox biology*, *41*, 101950. https://doi.org/10.1016/j.redox.2021.101950

96. Kanno, T., Nakajima, T., Kawashima, Y., Yokoyama, S., Asou, H. K., Sasamoto, S., Hayashizaki, K., Kinjo, Y., Ohara, O., Nakayama, T., & Endo, Y. (2021). Acsbg1-dependent mitochondrial fitness is a metabolic checkpoint for tissue Treg cell homeostasis. *Cell reports*, *37*(6), 109921. https://doi.org/10.1016/j.celrep.2021.109921

97. Semenza G. L. (2012). Hypoxia-inducible factors in physiology and medicine. *Cell*, *148*(3), 399–408. https://doi.org/10.1016/j.cell.2012.01.021

98. Sung, W. W., Chen, P. R., Liao, M. H., & Lee, J. W. (2017). Enhanced aerobic glycolysis of nasopharyngeal carcinoma cells by Epstein-Barr virus latent membrane protein 1. *Experimental cell research*, *359*(1), 94–100. https://doi.org/10.1016/j.yexcr.2017.08.005

99. Yogev, O., Lagos, D., Enver, T., & Boshoff, C. (2014). Kaposi's sarcoma herpesvirus microRNAs induce metabolic transformation of infected cells. *PLoS pathogens*, *10*(9), e1004400. https://doi.org/10.1371/journal.ppat.1004400
100. Jiang H. (2020). The complex activities of the SET1/MLL complex core subunits in development and disease. *Biochimica et biophysica acta. Gene regulatory mechanisms*, *1863*(7), 194560. https://doi.org/10.1016/j.bbagrm.2020.194560
101. Klonou, A., Chlamydas, S., & Piperi, C. (2021). Structure, Activity and Function of the MLL2 (KMT2B) Protein Lysine Methyltransferase. *Life (Basel, Switzerland)*, *11*(8), 823. https://doi.org/10.3390/life11080823
102. Zhou, P., Wang, Z., Yuan, X., Zhou, C., Liu, L., Wan, X., Zhang, F., Ding, X., Wang, C., Xiong, S., Wang, Z., Yuan, J., Li, Q., & Zhang, Y. (2013). Mixed lineage leukemia 5 (MLL5) protein regulates cell cycle progression and E2F1-responsive gene expression via association with host cell factor-1 (HCF-1). *The Journal of biological chemistry*, *288*(24), 17532–17543. https://doi.org/10.1074/jbc.M112.439729
103. Shi, Y., Wang, X. X., Zhuang, Y. W., Jiang, Y., Melcher, K., & Xu, H. E. (2017). Structure of the PRC2 complex and application to drug discovery. *Acta pharmacologica Sinica*, *38*(7), 963–976. https://doi.org/10.1038/aps.2017.7
104. van Mierlo, G., Veenstra, G. J. C., Vermeulen, M., & Marks, H. (2019). The Complexity of PRC2 Subcomplexes. *Trends in cell biology*, *29*(8), 660–671. https://doi.org/10.1016/j.tcb.2019.05.004
105. Barbour, H., Daou, S., Hendzel, M., & Affar, E. B. (2020). Polycomb group-mediated histone H2A monoubiquitination in epigenome regulation and nuclear processes. *Nature communications*, *11*(1), 5947. https://doi.org/10.1038/s41467-020-19722-9
106. Geng, Z., & Gao, Z. (2020). Mammalian PRC1 Complexes: Compositional Complexity and Diverse Molecular Mechanisms. *International journal of molecular sciences*, *21*(22), 8594. https://doi.org/10.3390/ijms21228594
107. Hyun, K., Jeon, J., Park, K., & Kim, J. (2017). Writing, erasing and reading histone lysine methylations. *Experimental & molecular medicine*, *49*(4), e324. https://doi.org/10.1038/emm.2017.11
108. Varga, J., Kube, M., Luck, K., & Schick, S. (2021). The BAF chromatin remodeling complexes: structure, function, and synthetic lethalities. *Biochemical Society transactions*, *49*(4), 1489–1503. https://doi.org/10.1042/BST20190960
109. Alfert, A., Moreno, N., & Kerl, K. (2019). The BAF complex in development and disease. *Epigenetics & chromatin*, *12*(1), 19. https://doi.org/10.1186/s13072-019-0264-y
110. Basta, J., & Rauchman, M. (2015). The nucleosome remodeling and deacetylase complex in development and disease. *Translational research : the journal of laboratory and clinical medicine*, *165*(1), 36–47. https://doi.org/10.1016/j.trsl.2014.05.003
111. Hoffmann, A., & Spengler, D. (2019). Chromatin Remodeling Complex NuRD in Neurodevelopment and Neurodevelopmental Disorders. *Frontiers in genetics*, *10*, 682. https://doi.org/10.3389/fgene.2019.00682
112. Park, S. Y., & Kim, J. S. (2020). A short guide to histone deacetylases including recent progress on class II enzymes. *Experimental & molecular medicine*, *52*(2), 204–212. https://doi.org/10.1038/s12276-020-0382-4
113. Hyndman, K. A., & Knepper, M. A. (2017). Dynamic regulation of lysine acetylation: the balance between acetyltransferase and deacetylase activities. *American journal of physiology. Renal physiology*, *313*(4), F842–F846. https://doi.org/10.1152/ajprenal.00313.2017
114. Padeken, J., Methot, S. P., & Gasser, S. M. (2022). Establishment of H3K9-methylated heterochromatin and its functions in tissue differentiation and maintenance. *Nature reviews. Molecular cell biology*, *23*(9), 623–640. https://doi.org/10.1038/s41580-022-00483-w
115. Zaghi, M., Broccoli, V., & Sessa, A. (2020). H3K36 Methylation in Neural Development and Associated Diseases. *Frontiers in genetics*, *10*, 1291. https://doi.org/10.3389/fgene.2019.01291
116. Sharda, A., & Humphrey, T. C. (2022). The role of histone H3K36me3 writers, readers and erasers in maintaining genome stability. *DNA repair*, *119*, 103407. https://doi.org/10.1016/j.dnarep.2022.103407

117. Zhang, X., Zhang, Y., Wang, C., & Wang, X. (2023). TET (Ten-eleven translocation) family proteins: structure, biological functions and applications. *Signal transduction and targeted therapy*, *8*(1), 297. https://doi.org/10.1038/s41392-023-01537-x
118. Zhao, R. Z., Jiang, S., Zhang, L., & Yu, Z. B. (2019). Mitochondrial electron transport chain, ROS generation and uncoupling (Review). *International journal of molecular medicine*, *44*(1), 3–15. https://doi.org/10.3892/ijmm.2019.4188
119. Miao, M., Chen, Y., Wang, X., Li, S., & Hu, R. (2025). The critical role of ferroptosis in virus-associated hematologic malignancies and its potential value in antiviral-antitumor therapy. *Virulence*, *16*(1), 2497908. https://doi.org/10.1080/21505594.2025.2497908
120. Grundlingh, J., Dargan, P. I., El-Zanfaly, M., & Wood, D. M. (2011). 2,4-dinitrophenol (DNP): a weight loss agent with significant acute toxicity and risk of death. *Journal of medical toxicology : official journal of the American College of Medical Toxicology*, *7*(3), 205–212. https://doi.org/10.1007/s13181-011-0162-6
121. Kudoh, A., Fujita, M., Zhang, L., Shirata, N., Daikoku, T., Sugaya, Y., Isomura, H., Nishiyama, Y., & Tsurumi, T. (2005). Epstein-Barr virus lytic replication elicits ATM checkpoint signal transduction while providing an S-phase-like cellular environment. *The Journal of biological chemistry*, *280*(9), 8156–8163. https://doi.org/10.1074/jbc.M411405200
122. Ramasubramanyan, S., Osborn, K., Flower, K., & Sinclair, A. J. (2012). Dynamic chromatin environment of key lytic cycle regulatory regions of the Epstein-Barr virus genome. *Journal of virology*, *86*(3), 1809–1819. https://doi.org/10.1128/JVI.06334-11
123. Piquet, S., Le Parc, F., Bai, S. K., Chevallier, O., Adam, S., & Polo, S. E. (2018). The Histone Chaperone FACT Coordinates H2A.X-Dependent Signaling and Repair of DNA Damage. *Molecular cell*, *72*(5), 888–901.e7. https://doi.org/10.1016/j.molcel.2018.09.010
124. Mai, J., Nazari, M., Stamminger, T., & Schreiner, S. (2025). Daxx and HIRA go viral - How chromatin remodeling complexes affect DNA virus infection. *Tumour virus research*, *19*, 200317. https://doi.org/10.1016/j.tvr.2025.200317
125. Zhu, F., Zhu, Q., Ye, D., Zhang, Q., Yang, Y., Guo, X., Liu, Z., Jiapaer, Z., Wan, X., Wang, G., Chen, W., Zhu, S., Jiang, C., Shi, W., & Kang, J. (2018). Sin3a-Tet1 interaction activates gene transcription and is required for embryonic stem cell pluripotency. *Nucleic acids research*, *46*(12), 6026–6040. https://doi.org/10.1093/nar/gky347
126. Flores, J. C., Sidoli, S., & Dawlaty, M. M. (2023). Tet2 regulates Sin3a recruitment at active enhancers in embryonic stem cells. *iScience*, *26*(7), 107170. https://doi.org/10.1016/j.isci.2023.107170
127. Lu, F., Wiedmer, A., Martin, K. A., Wickramasinghe, P. J. M. S., Kossenkov, A. V., & Lieberman, P. M. (2017). Coordinate Regulation of TET2 and EBNA2 Controls the DNA Methylation State of Latent Epstein-Barr Virus. *Journal of virology*, *91*(20), e00804-17. https://doi.org/10.1128/JVI.00804-17
128. Zhang, W., Han, D., Wan, P., Pan, P., Cao, Y., Liu, Y., Wu, K., & Wu, J. (2016). ERK/c-Jun Recruits Tet1 to Induce Zta Expression and Epstein-Barr Virus Reactivation through DNA Demethylation. *Scientific reports*, *6*, 34543. https://doi.org/10.1038/srep34543
129. Naipauer, J., Salyakina, D., Journo, G., Rosario, S., Williams, S., Abba, M., Shamay, M., & Mesri, E. A. (2020). High-throughput sequencing analysis of a "hit and run" cell and animal model of KSHV tumorigenesis. *PLoS pathogens*, *16*(6), e1008589. https://doi.org/10.1371/journal.ppat.1008589
130. Ghosh, A., Chandran, B., & Roy, A. (2025). IFI16 Mediates Deacetylation of KSHV Chromatin via Interaction with NuRD and Sin3A Co-Repressor Complexes. *Viruses*, *17*(7), 921. https://doi.org/10.3390/v17070921
131. Lavi, I., Bhattacharya, S., Awase, A., Orgil, O., Avital, N., Journo, G., Gurevich, V., & Shamay, M. (2025). Unidirectional recruitment between MeCP2 and KSHV-encoded LANA revealed by CRISPR/Cas9 recruitment assay. *PLoS pathogens*, *21*(3), e1012972. https://doi.org/10.1371/journal.ppat.1012972
132. Cai, Q., Cai, S., Zhu, C., Verma, S. C., Choi, J. Y., & Robertson, E. S. (2013). A unique SUMO-2-interacting motif within LANA is essential for KSHV latency. *PLoS pathogens*, *9*(11), e1003750. https://doi.org/10.1371/journal.ppat.1003750
133. Andrews S. (2010). FastQC: a quality control tool for high throughput sequence data. Available online at: http://www.bioinformatics.babraham.ac.uk/projects/fastqc

134. Dobin, A., Davis, C. A., Schlesinger, F., Drenkow, J., Zaleski, C., Jha, S., Batut, P., Chaisson, M., & Gingeras, T. R. (2013). STAR: ultrafast universal RNA-seq aligner. *Bioinformatics (Oxford, England)*, *29*(1), 15–21. https://doi.org/10.1093/bioinformatics/bts635

135. Patro, R., Duggal, G., Love, M. I., Irizarry, R. A., & Kingsford, C. (2017). Salmon provides fast and bias-aware quantification of transcript expression. *Nature methods*, *14*(4), 417–419. https://doi.org/10.1038/nmeth.4197

136. Ramírez, F., Ryan, D. P., Grüning, B., Bhardwaj, V., Kilpert, F., Richter, A. S., Heyne, S., Dündar, F., & Manke, T. (2016). deepTools2: a next generation web server for deep-sequencing data analysis. *Nucleic acids research*, *44*(W1), W160–W165. https://doi.org/10.1093/nar/gkw257

137. Love, M. I., Huber, W., & Anders, S. (2014). Moderated estimation of fold change and dispersion for RNA-seq data with DESeq2. *Genome biology*, *15*(12), 550. https://doi.org/10.1186/s13059-014-0550-8

138. Ge, S. X., Jung, D., & Yao, R. (2020). ShinyGO: a graphical gene-set enrichment tool for animals and plants. *Bioinformatics (Oxford, England)*, *36*(8), 2628–2629. https://doi.org/10.1093/bioinformatics/btz931

139. Kanehisa, M., & Goto, S. (2000). KEGG: kyoto encyclopedia of genes and genomes. *Nucleic acids research*, *28*(1), 27–30. https://doi.org/10.1093/nar/28.1.27

140. Gene Ontology Consortium, Aleksander, S. A., Balhoff, J., Carbon, S., Cherry, J. M., Drabkin, H. J., Ebert, D., Feuermann, M., Gaudet, P., Harris, N. L., Hill, D. P., Lee, R., Mi, H., Moxon, S., Mungall, C. J., Muruganugan, A., Mushayahama, T., Sternberg, P. W., Thomas, P. D., Van Auken, K., … Westerfield, M. (2023). The Gene Ontology knowledgebase in 2023. *Genetics*, *224*(1), iyad031. https://doi.org/10.1093/genetics/iyad031

141. Sander, W. J., Fourie, C., Sabiu, S., O'Neill, F. H., Pohl, C. H., & O'Neill, H. G. (2022). Reactive oxygen species as potential antiviral targets. *Reviews in medical virology*, *32*(1), e2240. https://doi.org/10.1002/rmv.2240

142. Kayesh, M. E. H., Kohara, M., & Tsukiyama-Kohara, K. (2025). Effects of oxidative stress on viral infections: an overview. *Npj viruses*, *3*(1), 27. https://doi.org/10.1038/s44298-025-00110-3

143. Foo, J., Bellot, G., Pervaiz, S., & Alonso, S. (2022). Mitochondria-mediated oxidative stress during viral infection. *Trends in microbiology*, *30*(7), 679–692. https://doi.org/10.1016/j.tim.2021.12.011